RESEARCH ARTICLE

Key Points:
- Eleven distal earthquakes over 23 years induced systematic hydrological responses throughout seven geoengineered schist landslides
- Observed responses are modulated by engineering but clearly dependent on spectral characteristics and energy of ground shaking
- The hydrologic system's ability to resist and recover from extrinsic perturbations is characterized using damped harmonic oscillator model

Spatially and temporally systematic hydrologic changes within large geoengineered landslides, Cromwell Gorge, New Zealand, induced by multiple regional earthquakes

Grant A. O'Brien[1,2] (ID)**, Simon C. Cox[3]** (ID)**, and John Townend[1]** (ID)

[1]School of Geography, Environment and Earth Sciences, Victoria University of Wellington, Wellington, New Zealand, [2]GNS Science, Institute of Geological and Nuclear Sciences Limited/Te Pū Ao, Lower Hutt, New Zealand, [3]GNS Science, Institute of Geological and Nuclear Sciences Limited/Te Pū Ao, Dunedin, New Zealand

Abstract Geoengineered groundwater systems within seven large (23×10^4–9×10^6 m^2), deep-seated (40–300 m), previously slow-creep (2–5 mm/yr.) schist landslides in the Cromwell Gorge responded systematically to 11 large ($M_w > 6.2$) earthquakes at epicentral distances of 130–630 km between 1990 and 2013. Landslide groundwater is strongly compartmentalized and often overpressured, with permeability of 10^{-17} to 10^{-13} m^2 and flow occurring primarily through fracture and crush zones, hindered by shears containing clayey gouge. Hydrological monitoring recorded earthquake-induced meter- or centimeter-scale changes in groundwater levels (at 22 piezometers) and elevated drainage discharge (at 11 V notch weirs). Groundwater level changes exhibited consistent characteristics at all monitoring sites, with time to peak-pressure changes taking ~1 month and recovery lasting 0.7–1.2 years. Changes in weir flow rate near instantaneous (peaking 0–6 h after earthquakes) and followed by recession lasting ~1 month. Responses at each site were systematic from one earthquake to another in terms of duration, polarity, and amplitude. Consistent patterns in amplitude and duration have been compared between sites and with earthquake parameters (peak ground acceleration (PGA), seismic energy density (e), shaking duration, frequency bandwidth, and site amplitude). Shaking at PGA ~0.27% g and $e \sim 0.21$ J m^{-3} induced discernable gorge-wide hydrological responses at thresholds comparable to other international examples. Groundwater level changes modeled using a damped harmonic oscillator characterize the ability of the system to resist and recover from extrinsic perturbations. The observed character of response reflects spectral characteristics as well as energy. Landslide hydrological systems appear most susceptible to damage and hydraulic changes when earthquakes emit broad-frequency, long-duration, high-amplitude ground motion.

1. Introduction

1.1. Earthquake Induced Hydrologic Responses

Large earthquakes induce a spectrum of both coseismic and post seismic hydrological responses, which have drawn scientific attention for their potential to elucidate information on crustal permeability and tectonic processes at spatial and temporal scales that are otherwise difficult to study [*Wang and Manga*, 2010]. The underlying processes are important because they are associated with hazards such as triggered seismicity, landslides, and liquefaction [*Hill et al.*, 1993; *Brodsky and Lajoie*, 2013; *Ellsworth*, 2013], geothermal and hydrocarbon resources [*Beresnev and Johnson*, 1994], the formation of mineral deposits [*Sibson*, 2001], and groundwater supplies [*Wang and Manga*, 2015] and the safety of nuclear waste repositories [*Carrigan et al.*, 1991]. Significant quantitative advances in "earthquake hydrology" have been made as more sites are instrumented and monitored, and the number and variety of earthquake responses have also increased. By developing empirical catalogues of earthquake-induced responses, it may be possible to elucidate underlying processes and driving mechanisms by testing hypotheses against time- and length-scale-appropriate observations [e.g., *Rojstaczer et al.*, 1995; *Roeloffs*, 1998; *Elkhoury et al.*, 2006, 2011; *Liu and Manga*, 2009; *Manga and Rowland*, 2009; *Wang and Manga*, 2010; *Cox et al.*, 2015]. To date, much research into earthquake-induced hydrologic phenomena has involved either data from a single site that span multiple earthquakes [*Roeloffs*, 1998; *Matsumoto et al.*, 2003; *Shi and Wang*, 2014; *Weingarten and Ge*, 2014] or data from many sites recording a single earthquake [*Wang et al.*, 2004b; *Chia et al.*, 2008; *Cox et al.*, 2012; *Yan et al.*, 2014]. A few studies have now started utilizing continent-wide records of multiple earthquakes at multiple sites

[*Parvin et al.*, 2014; *Shi et al.*, 2014, 2015a]. By eliminating variables, it may be possible to clarify the importance and interactions of various extrinsic (earthquake and tectonic), intrinsic (local hydrogeological), and anthropogenic (human-related) influences on responses observed.

Mechanisms commonly proposed to produce such hydrological changes are the movement of water due to poroelastic coupling associated with the redistribution of the stress field, undrained consolidation, or permeability changes associated with opening and closing of fractures and pore space. Observations made at different distances from earthquake epicenters are particularly suited for investigations of the relative roles of static and dynamic stress perturbations, as these stresses decay at different rates with distance and static stress changes are very small, or negligible, in the far field [*Wang and Manga*, 2010]. Persistent step-like changes in water level are common in the near field (less than one fault length from an earthquake's epicenter) and in many instances appear related to the static strain field induced by fault displacement [*Okada*, 1992; *Jónsson et al.*, 2003]. In the far field, by contrast, dynamic volumetric strains during the passage of seismic waves induce responses that are commonly attributed to permeability change, which can potentially be quantified through tidal analysis and strain measurements [*Burbey et al.*, 2012; *Elkhoury et al.*, 2006; *Shi et al.*, 2013; *Shi and Wang*, 2014; *Zhang et al.*, 2015]. Notably anomalous responses such as liquefaction observed "beyond near-field distances" [*Wang*, 2007] or wells particularly sensitive to earthquake-induced level changes [*Taira et al.*, 2009; *Weingarten and Ge*, 2014] often provide significant insight [*Manga et al.*, 2012].

The amplitudes and timescales of earthquake-induced hydrological responses exhibit substantial variation. In some cases, hydrological responses such as groundwater level oscillations (i.e., hydroseismographs), which mimic nearby seismological records, are short lived, lasting only 10^{-5}–10^{-1} days [*Blanchard and Byerly*, 1935; *Brodsky et al.*, 2003; *Weingarten and Ge*, 2014]. In contrast, stream flow rate increases, groundwater level changes, and changes in temperature or chemistry may persist for times of the order of 10^{2} days [*Roeloffs*, 1998; *Manga et al.*, 2003; *Elkhoury et al.*, 2006; *Cox et al.*, 2012; *Manga et al.*, 2012; *Wang and Manga*, 2015]. Observations of many long-lived, far-field hydrologic changes have been explained in terms of transient permeability enhancement within the groundwater system. Mechanisms proposed to explain this enhancement include the shaking loose of colloidal material and the unblocking of pore throats [*Roeloffs*, 1998; *Brodsky et al.*, 2003], pressure-induced permeability increase [*Roeloffs*, 1998; *Faoro et al.*, 2012], mobilization of a gaseous phase [*Beresnev and Johnson*, 1994; *Manga et al.*, 2012], and microfracturing [*Wang et al.*, 2004; *Manga and Rowland*, 2009]. Complimentary experimental work suggests the ionic strength of pore fluid can also influence permeability, and fluid chemistry may be coupled to small-scale particle mobility and enhanced permeability [*Candela et al.*, 2014]. The ability of these mechanisms to account for the eventual dissipation of the groundwater perturbations remains the subject of active scientific debate, and the extent to which pore- or fracture-scale changes are governed by coupling of mechanical or geochemical processes remains unclear [*Polak et al.*, 2004; *Wang and Manga*, 2010].

As yet, there are no clear relationships defining the extent to which different types of earthquake modulate triggering mechanisms and larger-scale processes. Attempts have been made to relate the amplitudes of hydrologic changes to measures of seismic shaking, including seismic energy density (e), peak ground acceleration (PGA), peak ground velocity (PGV), volumetric strain, and dynamic stress [*Elkhoury et al.*, 2006; *Wang*, 2007; *Wang and Manga*, 2010; *Cox et al.*, 2015; *Shi et al.*, 2015b]. At a single locality, the scale of responses tends to show a general correlation with earthquake magnitude and/or shaking amplitude, but when multiple sites are considered wide variations become evident. This suggests that local hydrogeological or structural conditions [*Cox et al.*, 2012; *Gulley et al.*, 2013; *Shi et al.*, 2013, 2015b], and even anthropogenic effects and observer interference [*Shi et al.*, 2015a], play important roles in controlling the amplitude and duration of responses observed. Seismic energy density (e), a parameter proportional to the dynamic strain associated with seismic waves, was proposed by *Wang and Manga* [2010] as a metric with which to discriminate the conditions under which different hydrological changes can be expected following earthquakes. In particular, they showed that increases in streamflow and liquefaction typically occur when seismic energy densities exceed 10^{-1} J m^{-3}, and in wells, more prolonged groundwater responses occur from 10^{-3} J m^{-3}.

1.2. This Study

Our study takes advantage of the extensive groundwater monitoring infrastructure installed to ensure slope safety at a large hydroelectric power facility, the Clyde Dam in central Otago, New Zealand. Geoengineering undertaken throughout the Cromwell Gorge in conjunction with the dam's construction reduced

groundwater levels to maintain slope stability above the impounded reservoir and monitoring records span more than two decades. We document and interpret hydrologic responses to multiple earthquakes recorded by multiple piezometers and underground weirs. Complementing the hydrological data are slope-movement data from extensometers; inclinometers; and survey marks, temperature, barometric, and operational data. In what is one of the most extensively and densely monitored long-duration field examples worldwide, albeit modified by anthropogenic activity, we document earthquake stimulation of a system with moderate- to low-permeability, fractured, compartmentalized hydrogeology. By focusing on this dense monitoring network, our study eliminates many of the intrinsic variables present in continent-wide investigations. Local (intrinsic) site effects are variably simplified and removed by normalizing response amplitude and duration. We use a damped harmonic oscillator model to characterize earthquake-induced hydrologic responses with regard to the system's ability to resist and recover from extrinsic perturbations. We argue that it is the ability of the hydrologic system to resist then recover from perturbations, which depends on spectral characteristics of shaking and not just the energy imposed on it, that affects the character of hydrological responses observed.

1.3. Study Area

Cromwell Gorge, in the central Otago region of the South Island, New Zealand (Figure 1) is the site of one of New Zealand's largest hydroelectric power generators, the 464 MW Clyde Dam. The gorge is 18 km long and bounded by pervasively foliated and fractured quartzofeldspathic schist interlayered with minor layers of metavolcanic greenschist [*Turnbull*, 1987; *Turnbull et al.*, 2001]. Lake Dunstan (the reservoir to the Clyde Dam) is impounded behind the 60 m high dam, occupying the floor of the Cromwell Gorge and extending a further 16 km upstream.

Seventeen large schist landslides (Figure 1) were mapped along the length of the gorge by *Turnbull* [1987]. These were studied further and progressively engineered during the dam construction (1976–1988), reservoir filling (1992–1993) and operational phases (1993 onward) to assess and mitigate movement [*Beetham and Fergusson*, 1990; *Gillon and Hancox*, 1991; *Macfarlane et al.*, 1991; *Thomson*, 1993]. Initially classified as "slow-creep" (2–5 mm yr^{-1}) landslides, geoengineering now controls and has all but halted their movement. A 16 km network of underground tunnels (Figures 1 and 2) with radially drilled drainage holes, penetrates the lower sections of the landslides and in situ schist beneath basal shear zones, close to present-day lake level (195 ± 1 m above sea level (asl)). The tunnels and drainage network artificially depress groundwater levels, lowering the potentiometric surface by more than 100 m in some areas, reducing pressures at the basal (and internal) shear zones and thereby stabilizing the slopes. Ongoing monitoring is carried out to ensure safety, using some 3500 instruments installed throughout the gorge, mostly concentrated on the lower land-slide sections. Although small accelerations have been recorded locally by extensometers and inclinometers in response to prolonged heavy rainfall, none appear to exhibit acceleration due to earthquakes or earthquake-induced hydrological responses (see supporting information). To our knowledge, there has been no significant landslide activity as a direct result of distal earthquake-induced changes that has required any operational mitigation.

Slow-creep landslides are common throughout the schist of central Otago, which is well-foliated, fissile, and weak [*Turnbull*, 1987]. In Cromwell Gorge, the landslides are laterally extensive and deep seated (40–300 m) and have formed within the schist bedrock, schist debris, and overlying colluvium [*Beetham and Fergusson*, 1990; *Gillon and Hancox*, 1991]. The landslides are more extensive on the eastern flank of the gorge, where foliation dipslopes provide failure surfaces on which landslides have developed. The largest landslide in the gorge, at Nine Mile Creek (Figure 1), is a complex slide encompassing an area of ~1200 ha and extending from below the present-day lake level at 195 m asl to near the top of the adjacent mountain range at 1646 m asl.

The landslides typically comprise four to five characteristic zones (Figure 2) that reflect varying degrees of rock disturbance (e.g., translation, rotation, shearing, buckling, and jointing) of the rock mass [*Beetham and Fergusson*, 1990]: chaotic and boulder debris (10^1–10^2 m displacement); block debris (10^0–10^1 m displacement); displaced schist (highly jointed and sheared, 10^{-3}–10^0 m displacement); disturbed schist (incipiently displaced, sheared, and rotated, and forming a transition zone between the landslide and subjacent basement, 10^{-3}–10^{-2} m displacement); and in situ schist (below slide basal zone, no landslide-induced displacement). The zones are commonly vertically stacked, but not every zone is present at any one locality.
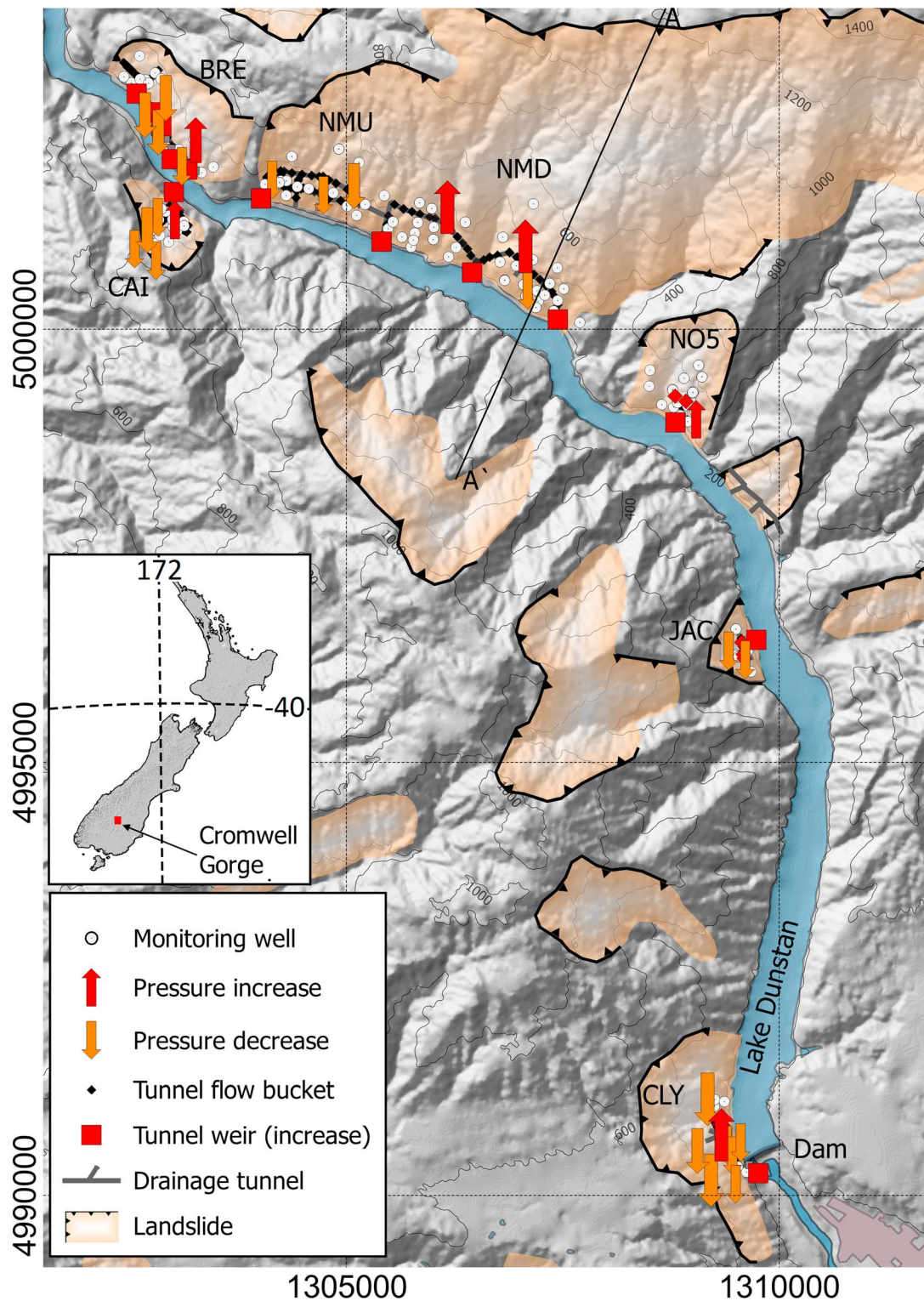
Figure 1. Map of landslides in the Cromwell Gorge, central Otago, South Island of New Zealand with an inset showing the location with respect to the rest of New Zealand. Map coordinates shown are in meters NZTM2000. The location of instruments recording hydrological data and the nature of the identified earthquake-induced responses are also shown: monitoring wells by grey circles, tunnel V notch weirs by squares, and tunnel flow buckets by grey diamonds; red markers (arrows, squares, and diamonds) indicate positive responses and orange markers indicate negative responses. The markers are scaled to reflect the approximate amplitude of change. Drainage tunnels, not specifically shown, can be located and visualized by the consecutive alignment of the tunnel flow bucket symbols. Landslides specifically referred to in the text have been labeled: BRE–Brewery Creek; NMU–Nine Mile Upstream; NMD–Nine Mile Downstream; NO5–Number 5; JAC–Jacksons; and CLY–Clyde.
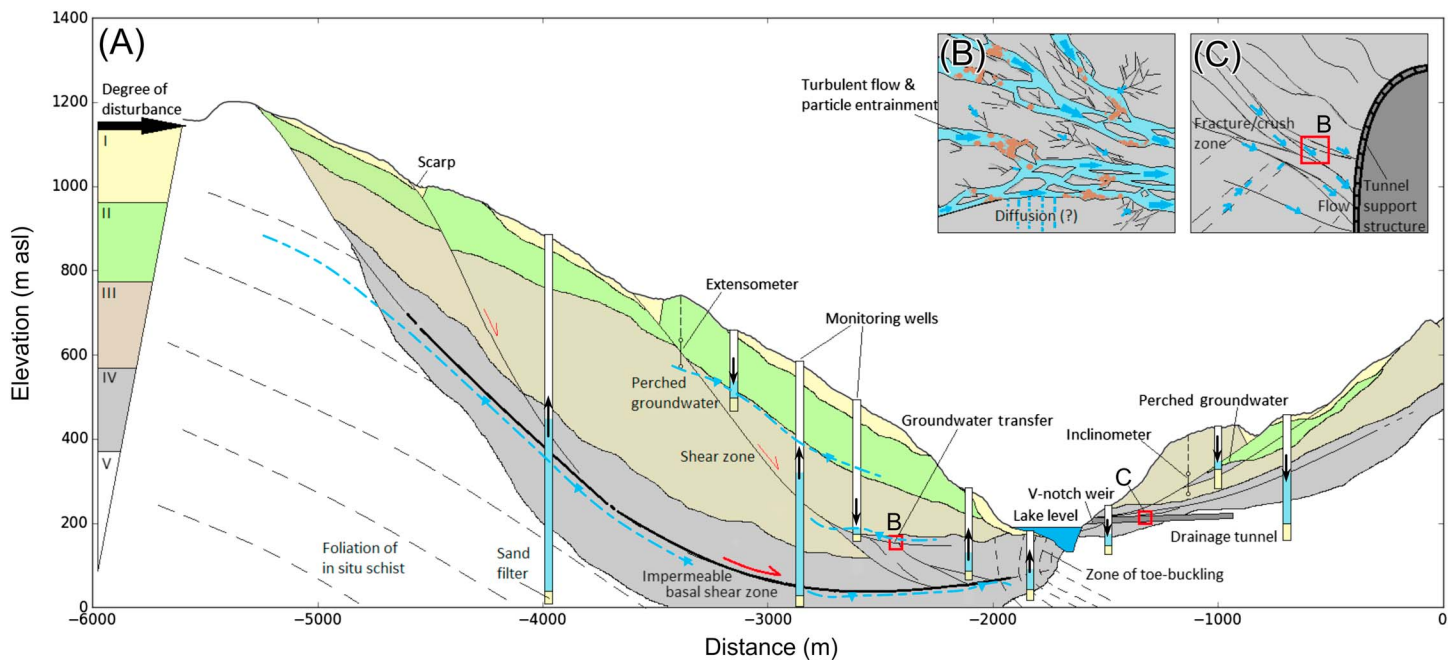
Figure 2. (a) Cross section depicting the hydrogeology typical of landslides in Cromwell Gorge, with conceptual hydrological effects stimulated by earthquakes. The topography is extracted from the cross-section A-A′ in Figure 1 to provide reference to the scale of the Nine Mile Downstream landslide. Rock-mass disturbance categories (I–V) have been adapted from *Beetham and Fergusson* [1990]. (b) Depiction at a fracture scale (mm–cm), of how earthquake stimulated groundwater flow may entrain and remove particulates in fractures, thereby temporarily increasing permeability/hydraulic conductivity (also applies to inset C). (c) Illustration at a meter scale, showing the groundwater flow from the rock mass into the tunnel systems.

The landslides also vary laterally in structure, particularly near their toes where large-scale toe buckling and internal thrusting have generated localized zones of open-jointed schist opposing zones of highly compressed and stressed schist [*Beetham and Fergusson*, 1990].

Observations made during drilling and subsequent tunneling reveal that the groundwater regime within each landslide is highly compartmentalized, and isotopic signatures and tritium dating suggest that the sub-basal groundwater has shorter residence times than landslide internal groundwater, which is on the order of 10^3 years [*Beetham and Fergusson*, 1990; *Macfarlane et al.*, 1991]. Hydraulic conductivities determined from >10,000 hydraulic head, slug, and packer tests vary between 10^{-10} and 10^{-6} m s^{-1}—that is, by 4 orders of magnitude—but with mean values of 10^{-7} m s^{-1} [*Beetham and Fergusson*, 1990; *Macfarlane et al.*, 1991; *Grocott et al.*, 1992]. However, the mean values and ranges calculated for landslide internal zones and underlying schist are all similar, corresponding to a mean permeability on the order of 10^{-14} m^2 (within a 10^{-17} to 10^{-13} m^2 range). The fractured reservoirs vary laterally and vertically, with perched, confined, and unconfined groundwater at different localities that are variably interconnected. Dry cavities and areas of significant over-pressure were encountered during drilling and tunneling. Compartmentalization of the groundwater regime is evident within the hydrological data.

1.4. Data Sets

In this study, data from 270 piezometers installed in boreholes to measure groundwater levels within and beneath the landslides and 45 subterranean V-notch weirs installed near tunnel exits to monitor rates of groundwater discharge (Figures 1 and 2) are analyzed in order to understand how the geoengineered landslides respond to repeated earthquake-induced shaking. Hydrological data (examples shown in Figure 3) have been recorded since 1990 at sampling intervals of between 1 and 24 h (2.7×10^{-4} to 1.16×10^{-5} Hz). These data are augmented by outcrop measurements; core; trench; and tunnel surface descriptions, extensometer, and inclinometer data (3-hourly; 9.25×10^{-5} Hz), hydrological test pit, and borehole packer/slug tests.

The central Otago region is one of the driest parts in New Zealand, with the nearby town of Alexandra recording average annual rainfall of 340 mm [*Wilson and Lu*, 2011]. This relatively low rate of
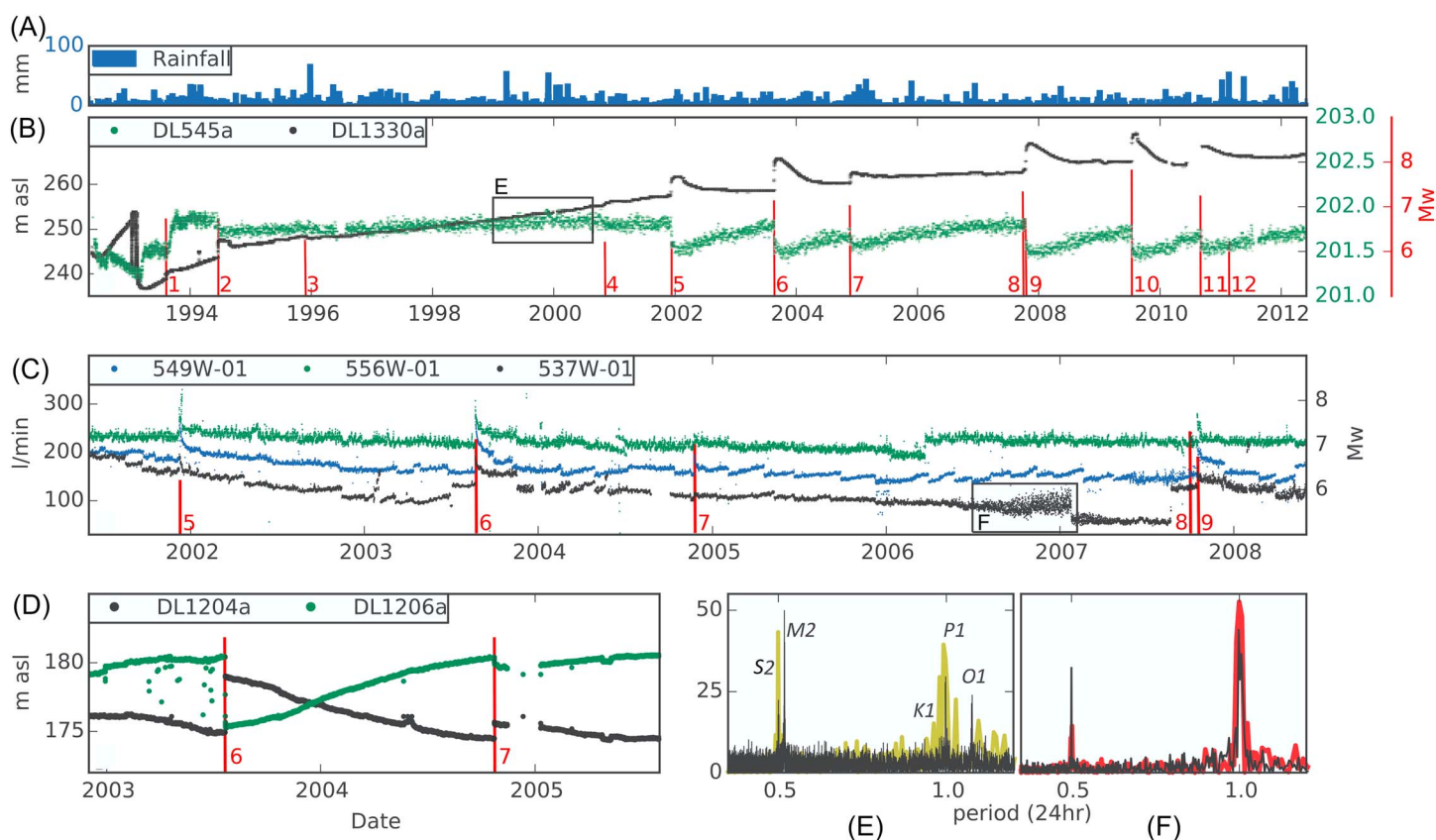
Figure 3. Examples of hydrological data recorded in Cromwell Gorge. (a) Local rainfall recorded by the Clyde Electronic Weather Station. (b) Groundwater level (piezometer) data from monitoring wells DL545a (black) and DL1330a (green) in the Nine Mile Downstream landslide. The timing of the 12 earthquakes studied (numbered 1–12; refer to Figure 4) are shown by vertical red bars with height that corresponds to earthquake magnitude. (c) Examples of data from tunnel V notch weirs located in Nine Mile Creek Downstream slide area and No. 5 Slide. (d) Groundwater level data from two wells 95 m apart in the Clyde landslide where earthquake-induced perturbations appear to mirror each other. (e and f) The spectra (periodograms) of small period oscillations with groundwater level (DL545a) and discharge data (537 W-01), computed from the inset boxes on plots B and C.

precipitation aids in the characterization of earthquake-induced hydrologic changes, but there have nevertheless been large rainfall events during the >20 year period addressed by this study (Figure 3). These include 6 of the 10 largest rainfall events recorded in the area since 1950 [*Macfarlane*, 2009]. Some portions of landslides in Cromwell Gorge (e.g., Cairnmuir Slide or a section of the Brewery Creek Slide) have been observed to accelerate over months to years in response to heavy rainfall [*Gillon et al.*, 1991; *Macfarlane*, 2009], and, as discussed below, the hydrologic changes associated with rainfall can be readily distinguished from earthquake-induced changes. Rainfall records from the Clyde weather station located approximately 2.7 km south of the dam have been obtained from http://cliflo.niwa.co.nz/ (last accessed 1 April 2016).

Most of the seismological data used in this study were recorded at four stations (Figure 4 and Table 1) in operation at different times. The permanent national network (GeoNet) station closet to the Cromwell Gorge, Earnscleugh (EAZ), is approximately 6 km south of the Clyde Dam. It consists of a broadband seismometer and a strong-motion sensor but has only been in operation since 1 November 2004. The next closest station, located at Alexandra (AXZ) approximately 9 km southeast of the dam, was operated between 7 March 1996 and 31 August 2004, and utilized a short-period (L4C-3D) sensor. Some data from the permanent Wanaka (WKZ) broadband national network station, 47 km northwest of the dam and in operation since 3 June 2004, have also been used. The nearest station that has been in operation throughout the period of interest, since 1990, is located in Milford Sound (MSZ), approximately 122 km west of the dam. MSZ is too far away to provide useful records of ground shaking in Cromwell Gorge but is useful as a measuring standard as it recorded all of the large regional earthquakes of interest in this study. Data from a private
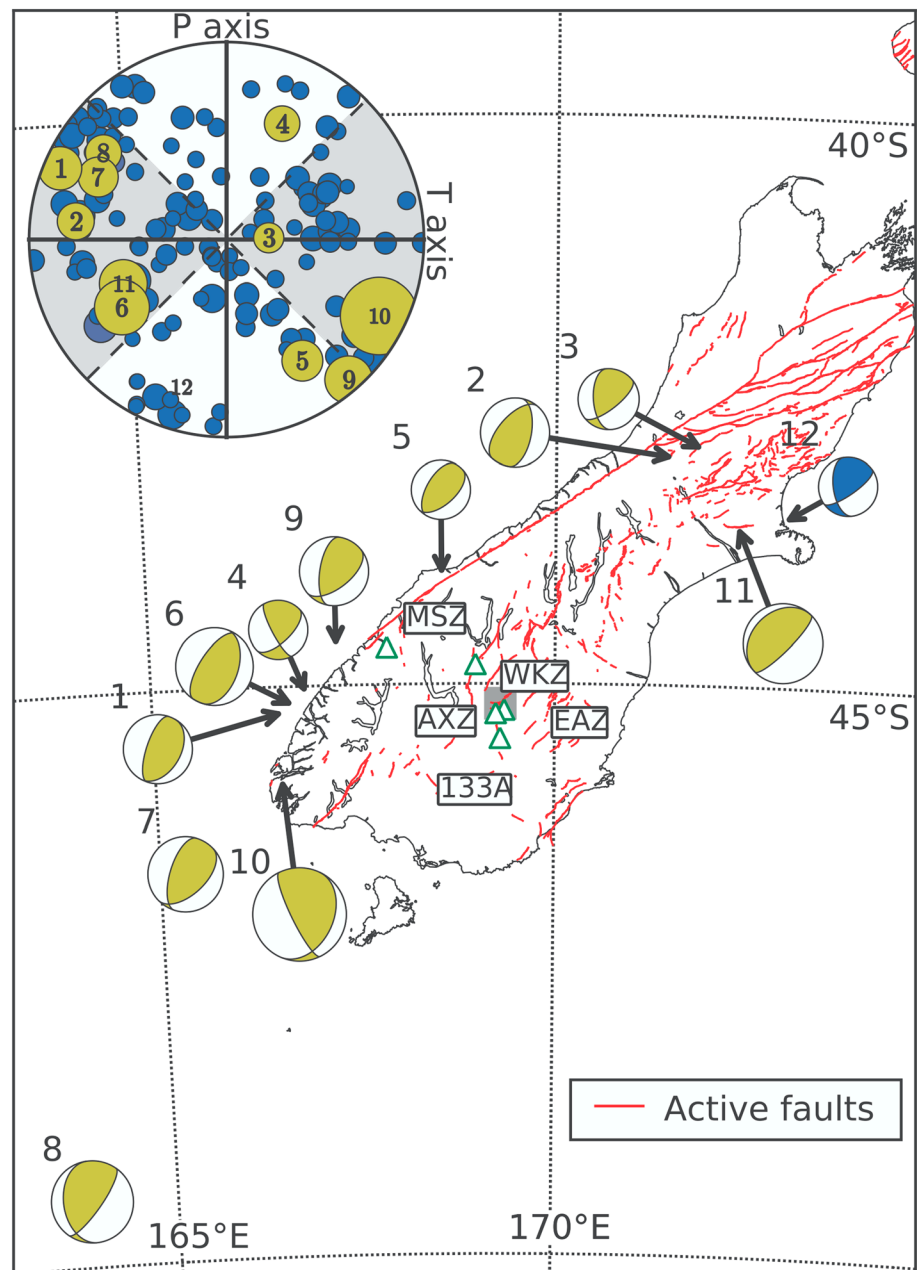
Figure 4. The 12 earthquakes associated with the hydrologic changes within Cromwell Gorge landslide groundwater systems. Earthquake locations are shown by the black arrows and numbered (1–12) focal mechanisms (lower hemisphere stereonets; T quadrants shaded) are scaled to depict the earthquake magnitude. Yellow focal mechanisms represent earthquakes associated with gorge-wide hydrologic changes whereas the blue focal mechanism (the 2010 M_w6.2 Christchurch earthquake studied for comparison) does not associate with any hydrologic changes in Cromwell Gorge. The location of Cromwell Gorge (and extent of Figure 1) is shown by the grey box. Seismometers and strong-motion instruments used in this study are shown by the labeled triangles and known active faults with red lines [*Langridge et al.*, 2016]. The circular inset (upper left) is a normalized focal mechanism plotting all recorded New Zealand earthquakes since 1991 that were $> M_w5$; here earthquake takeoff angles are plotted as north-east down equaling the *P*, *T*, and *N* focal axes respectfully. Numbered yellow and blue markers correspond to the earthquakes shown in the main figure.

strong-motion station (133A) operated by the Roxburgh Dam (33 km south of the Clyde Dam) have also been investigated. All waveform data were downloaded directly from GeoNet (http://www.geonet.org.nz/, last accessed 1 April 2016) and earthquake focal mechanism data (Figure 4) from the references listed in the Table 2 footnote.

Table 1. New Zealand Seismometer Stations (Operated by GeoNet; See www.Geonet.org.nz) Used in This Study, Listing Unique Identifier Codes, Periods of Operation, and Distances to the Study Site

GeoNet Station	Operational Period	Distance to Site (km)
EAZ	1/11/2004 (ongoing)	6
AXZ	7/3/1996–31/8/2004	9
133A	20/6/1995–23/3/2004	33
MSZ	3/3/1966 (ongoing)	122

2. Method and Data Analysis

2.1. Characterization of Hydrological Signals

The hydrological data set contains discernable signals produced by a broad range of climatic, tidal, anthropogenic, and earthquake processes (Figure 3). Climatic signals encompass short- and long-term, rainfall-related groundwater recharge, discharge, and recovery and are readily identified using local rainfall measurements. Some monitoring sites also exhibit seasonal fluctuations with higher groundwater levels and greater flow rates during the spring and autumn months associated with snow melt and more frequent rainfall, respectively.

The typical scale of rainfall-related signals is quite distinct from that of earthquake-related anomalies; for example, in weir data, the discharge responses to rainfall are often smaller in amplitude (by a factor of 5) and of much longer duration (time to peak flow rate higher by a factor of 200 and recession time higher by a factor of 8) than inferred earthquake-related responses. Fortuitously, sensors that recorded strong earthquake-related influences tend to show only minor rainfall-related effects, if any (e.g., sensors DL545a and 549 W-01; Figures 3b and 3c).

Groundwater oscillations corresponding to Earth tides and barometric pressure changes occur with amplitudes of tens of millimeters throughout much of the hydrological data set, notably in monitoring well DL1330a within the Nine Mile Downstream slide area (Figures 1, 3b, and 3e). The effects of Earth tide-related and barometric signals were identified in the frequency domain (e.g., Figure 3e), and, where necessary, the signals were removed using appropriate frequency filters and a predictive Bayesian modeling procedure implemented in the Baytap08 software [*Tamura et al.*, 1991; *Tamura and Agnew*, 2008].

The phase lags between periodic hydrological signals and calculated Earth tide stresses and changes in these lags following earthquakes or other perturbations have been used elsewhere to estimate hydrologic systems' permeability [*Elkhoury et al.*, 2006; *Burbey et al.*, 2012]. Preliminary work on Earth tide signals has been undertaken using the Cromwell Gorge data set [*O'Brien*, 2014] but is not presented here. Flow across one of the tunnel weirs (537 W-01) in the No. 5 Slide exhibits a strong correlation with local air temperatures (spectrum shown by Figure 3f), outside periods of rainfall recharge, suggesting that this landslide's permeability and/or internal stress may vary on a diurnal basis. Further work, beyond the scope of this paper, is required to fully document and interpret these periodic changes in hydrologic parameters.

Table 2. Earthquakes Analyzed in This Study, Listing Date and Time in UTC, Magnitude, Epicenter Location, Centroid Depth, Strike/Dip/Rake (S/D/R), Epicentral Distance to the Study Site, Location of the Takeoff Angle (TOA) on a Normalized Focal Sphere (Where C = Compressional, D = Dilatational, NP = Near Nodal Plane, and N = Near Null Axis), Measured PGA at EAZ or Derived *PGAc* (Using Equation (1)) and Seismic Energy Density *e* (Equation (2))

Name	No.	Date and Time (UTC)	M_w	Epicenter	Depth (km)	S/D/R[a]	Distance (km)	TOA	PGA or *PGAc* (% g)	*e* (J/m^3)
Fiordland	1	10/8/1993 0:51	6.7	−45.21, 166.71	5	030/30/100	204	C	*0.88*	0.32
Arthurs Pass	2	18/6/1994 3:25	6.7	−43.01, 171.48	4	221/47/112	297	C	*0.51*	0.22
Cass	3	24/11/1995 6:18	6.3	−42.95, 171.82	7	176/45/44	319	C	*0.34*	0.13
Thompson Sound	4	1/11/2000 10:35	6.2	−45.12, 166.95	9	171/57/59	185	D	*0.69*	0.20
Jackson Bay	5	7/12/2001 19:27	6.2	−44.11, 168.61	5	048/45/103	131	D[a]	*1.08*	0.29
Secretary Island	6	21/8/2003 12:12	7.2	−45.19, 166.83	24	020/35/79	195	C[a]	*1.17*	0.47
Puysegur04	7	22/11/2004 20:26	7.1	−46.61, 165.32	12	046/41/113	348	C	0.27	0.29
Puysegur07	8	30/9/2007 5:23	7.3	−49.42, 163.84	10	035/70/108	627	C[a]	0.10	0.20
George Sound	9	15/10/2007 12:29	6.7	−44.72, 167.30	20	052/46/123	166	D[a]	1.45	0.39
Dusky Sound	10	15/7/2009 9:22	7.8	−45.75, 166.58	15	026/24/140	223	C	0.81	0.99
Darfield	11	3/9/2010 16:35	7.1	−43.54, 172.16	8	226/017/91	292	C	0.44	0.35
Christchurch	12	21/2/2011 23:51	6.2	−43.57, 172.69	4	055/66/129	324	D	0.14	0.12

[a]References: All magnitude and epicenter data sourced from GeoNet (www.geonet.org.nz). Earthquake focal mechanism references are as follows: 1 = *van Dissen et al.* [1994]; 2 = *Abercrombie et al.* [2000]; 3 = *Gledhill et al.*, [2000]; 4 = *Robinson et al.* [2003]; 5 = *McGinty et al.* [2005]; 6 = *Reyners et al.* [2003]; 7,8 = GeoNet; 9 = *Petersen et al.* [2009]; 10 = *Fry et al.* [2010]; 11 = *Gledhill et al.* [2010]; 12 = *Kaiser* et al., [2012].
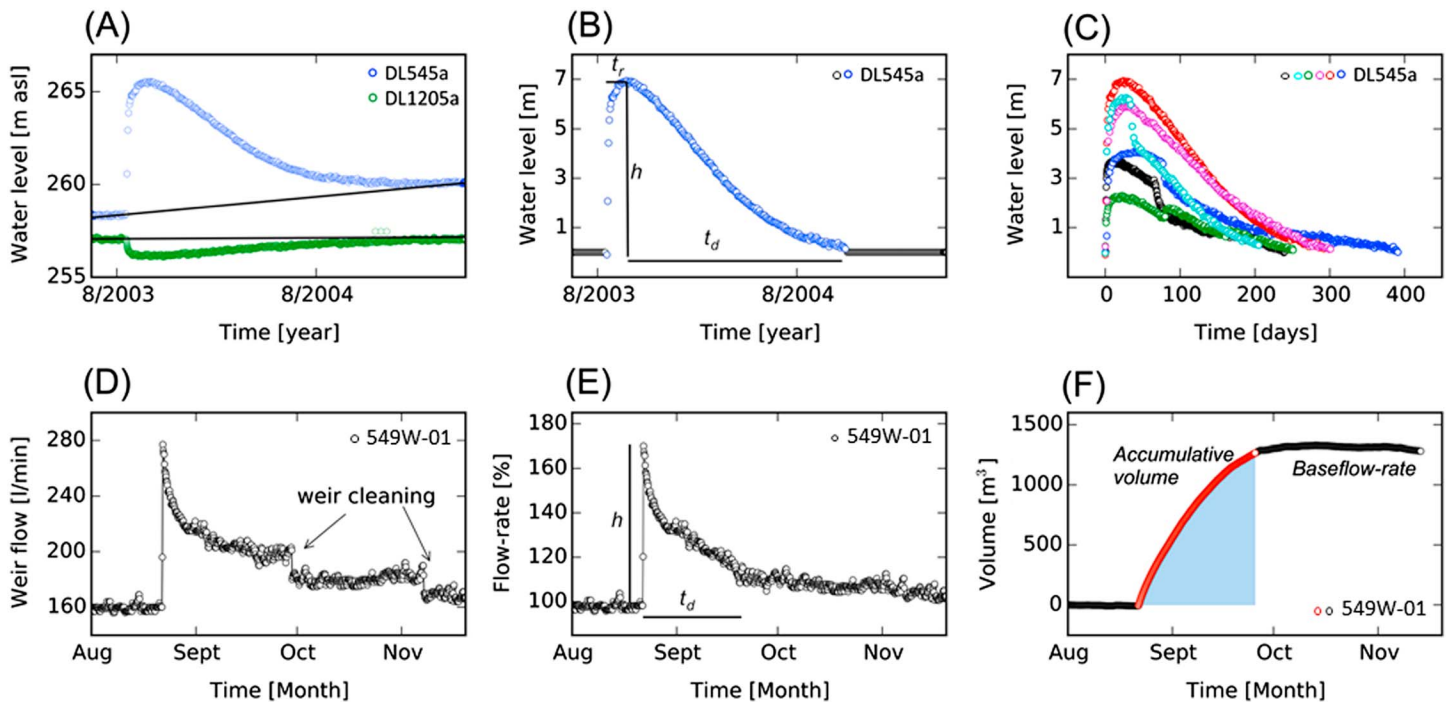[b]*PGAc*: Derived values are those with italic numerals.

Figure 5. Methodology for measuring earthquake-induced hydrologic responses within monitoring well (piezometer) and weir data. (a) Piezometer data immediately before, during, and after the 2003 M_w7.0 Secretary Island earthquake from DL545 (Nine Mile Downstream slide area) in blue and DL1205a (Clyde Slide) in green. The long-term trends within the hydrological data are shown by black lines of which the earthquake-induced signals appear superimposed. (b) Earthquake-induced hydrological response to the 2003 M_w7.0 Secretary Island earthquake after filtering for other hydrological signals, measuring lines show how the responses were quantified and characterized. (c) All earthquake-induced hydrologic responses at DL545a post processing, with their initiation time normalized to zero. (d) Weir data from 549 W-01 (Nine Mile Downstream) with weir cleaning event identified. (e) Weir data after removal of the effect of cleaning with marker lines showing how they were quantified and characterized. (f) Illustration of the calculation for the accumulative volume of excess discharged groundwater.

The anthropogenic influences most easily recognized are marked by impulsive decreases and subsequent partial recoveries in piezometric levels during the engineering phases when tunnels were first excavated and hill slopes drained just before the lake was filled. Following the initial drawdown and partial recovery of the water table, many monitoring wells exhibit a long-term "background trend" with slowly increasing, slowly decreasing, or stable piezometric levels. Large, rapid fluctuations in flow rate recorded in weirs during tunneling and drilling operations as compartmentalized groundwater was penetrated and released are followed by either slowly decreasing or substable flow rates (Figures 3b, 3c, and supporting information). Background trends are interpreted to reflect slow changes in the efficiency of the tunnel/drill hole drainage network, caused either by chemical precipitation of calcite and clay minerals or possibly by shear-induced obstruction and small amounts of otherwise undetected landslide displacement.

A subordinate anthropogenic effect on weir flow rates is the repeated maintenance of weirs. Weirs are cleaned periodically of accumulated debris and calcite precipitate (which otherwise bias flow rates upward due to the displacement of water), inducing small negative steps in the flow rate (e.g., weir 549 W-01; Figures 3c and 5d). The effects of cleaning events are easily identified from operational records, and corrections were applied assuming a linear accumulation rate of debris/precipitate.

Once climatic, tidal and anthropogenic anomalies have been identified, distinct positive and negative groundwater level changes, and increased groundwater discharge associated with large intermediate and far-field earthquakes can be readily identified (Figures 3–5). The amplitudes of the observed earthquake-related groundwater level responses are of the order of 10^{-2} to 10^{1} m (i.e., centimeters to meters in scale), which include many >1 m scale responses that are relatively large in comparison to previously reported international examples of intermediate and far-field responses [e.g., *Brodsky et al.*, 2003; *Chia et al.*, 2008; *Roeloffs*, 1998; *Shi et al.*, 2014, 2015a]. The durations of the groundwater level changes, persisting for several months to more than a year, are also relatively long.

In order to extract earthquake-related signals from long-term hydrological trends (when present), polynomial functions were fitted to the data. An extracted example of an earthquake-related water level change, and the polynomial function fitted to the long-term data beyond the scale of the graph, is provided in Figure 5a. Such polynomials represent background trends and subtracted from the data to isolate the earthquake-related signals of interest.

The earthquake-related groundwater level changes recorded by piezometers have been quantified in terms of (1) the amplitude to peak-pressure change, (2) the time to peak-pressure change, (3) the recovery time, and (4) the net earthquake-induced offset (if any). Earthquake-induced changes in weir flow rate have been characterized in terms of (5) the time to peak flow rate, (6) the recession time, (7) the percentage of increase in flow, and (8) the total volume of groundwater discharged in excess of base flow. Data are provided in Table S1 in the supporting information.

To examine the degree of consistency within the hydrological signals, the groundwater level changes and flow rate increases corresponding to each earthquake were correlated and ranked by amplitude against others at each site (i.e., groundwater level changes with groundwater level changes and flow rate with flow rate), using a pairwise Spearman rank-order correlation [*Daniel*, 1990] (see also section 3). The Spearman rank-order correlation matrices reveal whether the earthquake-induced network-wide responses are consistent or random: that is, the degree to which the network-wide responses are consistent in amplitude for each earthquake. The statistical analysis is performed separately for piezometer measurements of groundwater level changes and for the weir measurements of flow rate increases and then for the two data types combined.

2.2. Seismological Analysis

The seismometer closest to Cromwell Gorge that has been in operation throughout the period spanned by the hydrological data is MSZ located in Milford Sound approximately 120 km west of the gorge. MSZ is close to the epicenters of many earthquakes that triggered responses in the Cromwell Gorge landslides and is used here to obtain a homogeneous (albeit distant) set of peak ground acceleration (PGA) measurements, which are then used to calibrate the incomplete set of recorded PGA values at sites nearer the gorge (EAZ, AXZ, and WKZ; Figure 4).

PGA is a commonly used measure of earthquake shaking-intensity at hard-rock sites [*Wylie*, 1995; *Zhao et al.*, 1997]. To complete a catalogue of PGA measurements likely experienced at Cromwell Gorge during earthquakes prior to 2004, horizontal PGA_h and vertical PGA_v values were extrapolated from MSZ to the EAZ site using the following decay model:

$$\log(PGAc[\%g]) = c_1 + c_2 M_w - c_3 \, \log(D[km]) \tag{1}$$

Here $c_1 = 2.175$, $c_2 = 0.765$, and $c_3 = 1.398$ are constants derived from the regression of data at EAZ, M_w is moment magnitude, and D is the epicentral distance measured in kilometers. PGAc values in the horizontal and vertical directions were scrutinized and compared with values generated by the previously published New Zealand PGA attenuation model of *Zhao et al.* [1997], yielding comparable results.

Seismic energy density (*e*) provides an indication of the dynamic strain associated with seismic waves and the potential energy available to do work on a unit volume of rock [*Lay and Wallace*, 1995; *Brodsky et al.*, 2003]. It can also be used in addition to characterize the effects of seismic waves and to provide a comparison with previously reported earthquake-induced hydrological responses elsewhere [*Wang and Manga*, 2010]. Seismic energy density can be calculated using the empirical relationship [after *Wang*, 2007]

$$\log e \left[J/m^3 \right] = -3 \log D [km] + 1.45 M_w - 4.24 \tag{2}$$

Directivity effects, radiation patterns, and nonuniform attenuation structures are not taken into account in this formulation of seismic energy density, despite their likely importance for some of the earthquakes under analysis. The 2009 M_w7.8 Dusky Sound earthquake, for instance, ruptured toward the south-southwest, away from Cromwell Gorge, such that relatively low accelerations and shaking intensities were experienced across the South Island given the large moment of this earthquake [*Fry et al.*, 2010]. The effects of radiation patterns (i.e., position on the focal sphere) are considered below, but otherwise, the empirical relationship for seismic energy density is used without modification.

In order to gain an understanding of the effects of the spectral content and shaking duration felt at the site, earthquakes were examined and characterized using continuous wavelet transforms [*Gurley and Kareem*, 1999]. Continuous wavelet transforms using a Morlet wavelet were applied to the accelerometer data (after removal of the instrument responses) with a function parameter of eight, to obtain accurate resolution of frequencies in the 10^{-2}–10^1 Hz bandwidth of interest [*de Moortel et al.*, 2004].

2.3. Damped Harmonic Oscillator Modeling

A damped harmonic oscillation (DHO) model is utilized here to numerically interpret earthquake-induced groundwater level changes. Damped oscillators are used to control (absorb) the energy from slow and fast impacts (i.e., compression damping and automotive shock absorbers) and then exhibit controlled recovery (i.e., rebound damping) to a prestimulated condition [*Wylie*, 1995]. The numerical definition of damped harmonic oscillation provides a means of modeling and comparing hydrologic responses that are similar in shape but operate on different amplitude and time-scales. The DHO can be represented mathematically as

$$\frac{d^2x}{dt^2} + 2\,\zeta\omega_0\,\frac{dx}{dt} + \omega_0^2 x = 0 \tag{3}$$

where x represents the amplitude of change, t the duration, ζ the assumed damping ratio, and ω_0 the natural period of the oscillator [*Wylie*, 1995]. The damping ratio is a dimensionless number that represents how effectively a system can resist and recover from change: a damping ratio less than one represents an under-damped system in which oscillatory motion is attenuated over several cycles (e.g., hydroseismographs); a damping ratio of one represents a critically damped, nonoscillatory system that returns to the prestimulated level monotonically; and a damping ratio greater than one represents persistent, exponential decay.

3. Results

3.1. Hydrological Changes Associated With Regional Earthquakes

Earthquake-induced responses can be discerned in the majority of records from the 315 hydrological instruments throughout the gorge, but only 22 monitoring wells and 11 V notch weirs recorded data with sufficient sampling rate fidelity and continuity to be useful for modeling. These 22 monitoring wells and 11 weirs recorded distinct changes in groundwater levels and increases in groundwater discharge in response to the same 11 intermediate to far-field (130–630 km) earthquakes (Figures 1, 3, and 4). The onsets of groundwater level change and increased tunnel discharge both occurred abruptly (Figures 3 and 4); however, the hydrological data set's minimum prolonged sampling interval of 3 h precludes identifying the changes as strictly coseismic. No hydrological responses to teleseismic earthquakes have been detected to date at this location.

Groundwater level changes in each of the 22 monitoring wells were consistently either of meter scale, decimeter scale, or centimeter scale. For example, groundwater level changes in DL545a (NMD Slide Area, Figure 3) spanned 1.3–6.9 m, in DL647 (BRE Slide) spanned 0.12–1 m, and in DL790a (JAC Slide) spanned 0.10–0.16 m. V notch weir flow rates increases ranged from 10% to 230% across the 11 weirs (Figure 1), and as an example, excess water (i.e., above base flow rate) released out each tunnel in NMD slide area alone ranged from 4 to 1040 m³. Monitoring wells vary in depth, with sand packers being located within a landslide zone or penetrating into in situ schist below the basal shear zone (Figure 2). The meter scale, decimeter scale, or centimeter scale amplitude scales of groundwater level changes generally correspond to deep (200–300 m) subbasal wells, lower zone (III and IV) landslide-internal wells or shallow upper zone (I and II) landslide-internal wells, respectively.

Of the 11 earthquakes inducing hydrological responses (Table 2), 8 produced responses that could be readily correlated between the 22 piezometers and 11 weir sites throughout the network-wide extent of the gorge (e.g., Figure 3). The analysis below is focused on these eight earthquakes. The responses to the remaining three earthquakes (1995 M_w6.3 Cass, 2000 M_w6.2 Thompson Sound, and 2007 M_w7.3 Puysegur) were not network wide, being either too small in some locations to be clearly distinguishable from other hydrological signals or not recorded due to instrument faults. These events are incorporated in the earthquake analysis but excluded from modeling. The Christchurch M_w6.3 2011 earthquake, which caused 185 fatalities and extensive damage to the city of Christchurch and surrounding areas [*Reyners*, 2011; *Kaiser et al.*, 2012], did not produce any measurable responses in Cromwell Gorge, but as it occurred at similar distances to those earthquakes
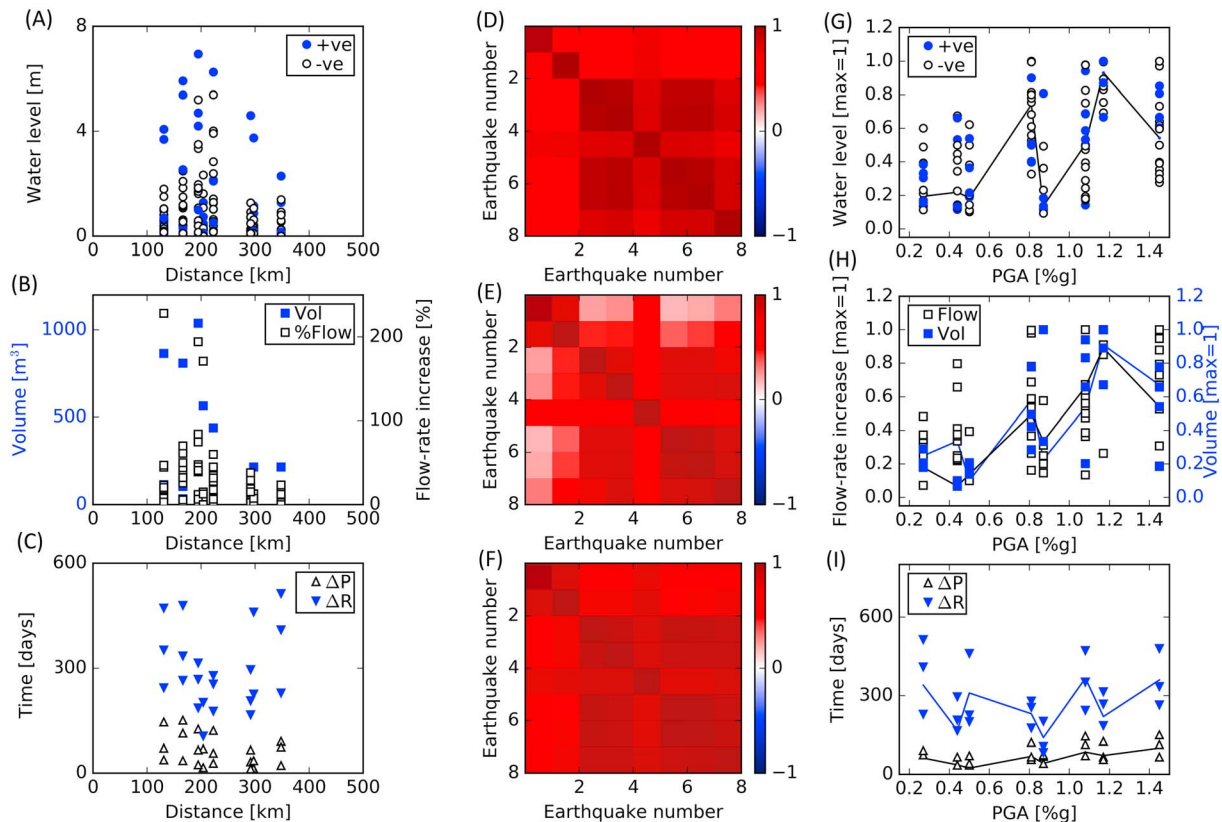
Figure 6. (a) Absolute (positive: blue; negative: white) groundwater level changes against epicentral distance. (b) Flow rate increases (white marker; as a percent increase) and accumulated excess volume (blue marker) against epicentral distance. (c) Time to peak pressure changes (ΔP) and recovery time (ΔR) of groundwater level changes, plotted against epicentral distance. The similarity of the response of the network to each earthquake is shown via Spearman rank-order correlation matrices for (d) monitoring wells, (e) V notch weirs, and (f) all sensors, where 1 is a perfect correlation and -1 is no correlation. (g) Normalized, absolute (positive: blue; negative: white) groundwater level changes against PGA (peak ground acceleration in % g where g is gravitational acceleration taken to be 9.89 m s^{-2}. (h) Normalized flow rate increases (white marker; from percent increase) and accumulated excess volume (blue marker) against PGA. (i) Time to peak pressure changes (ΔP) and recovery time (ΔR) of groundwater level changes, plotted against PGA. Black and blue lines in (g, h, and i) connect mean values determined for each earthquake.

that did has been analyzed here as an example of a high-energy (PGA$_v$ 220% g and PGA$_h$ 170% g near the epicenter), high-stress drop event [*Fry and Gerstenberger*, 2011; *Reyners*, 2011; *Kaiser et al.*, 2012].

At each monitoring site, the observed earthquake-induced hydrological responses exhibit systematic characteristics (Figures 3 and 5–7). Weir data uniformly exhibit abrupt increases in flow rates, with the amplitude of the increase reflecting the local groundwater availability, shown by the base flow rates. In other words, tunnels with a greater base flow rate discharged greater volumes of earthquake-mobilized water than tunnels with lower base flow. The proportional increase in flow rate is therefore considered a more representative indicator of earthquake effects than the corresponding absolute value. The times taken to reach peak flow rates were typically on the order of 0–6 h and were followed by recession periods lasting of the order of 1 month.

Piezometer data reveal similarly consistent patterns but with the difference that groundwater levels are observed to systematically increase at some sites and to systematically decrease at others (e.g., Figure 3d). Each site exhibits consistency in the range of amplitudes it records, which varies between sites: earthquake-induced groundwater level changes at some sites vary on a centimeter scale and at other sites on a meter scale. The groundwater levels also reach peak levels (peak-pressure changes) on consistent time periods. For example, groundwater level changes in monitoring well DL545a (subbasal, Nine Mile Downstream slide area) are always positive, always occur on a meter scale, with a time to peak-pressure change on the order of 2–3 weeks and a recovery time on the order of 0.7–1.0 years (Figures 3b, 5, and 6). Conversely, groundwater level changes in DL1330a (landslide internal, Nine Mile Downstream slide area) are consistently negative, occur on a centimeter scale, and exhibit a time to peak-pressure change on the order of 8–9 weeks, followed by a subsequent recovery over 0.7–1.2 years.
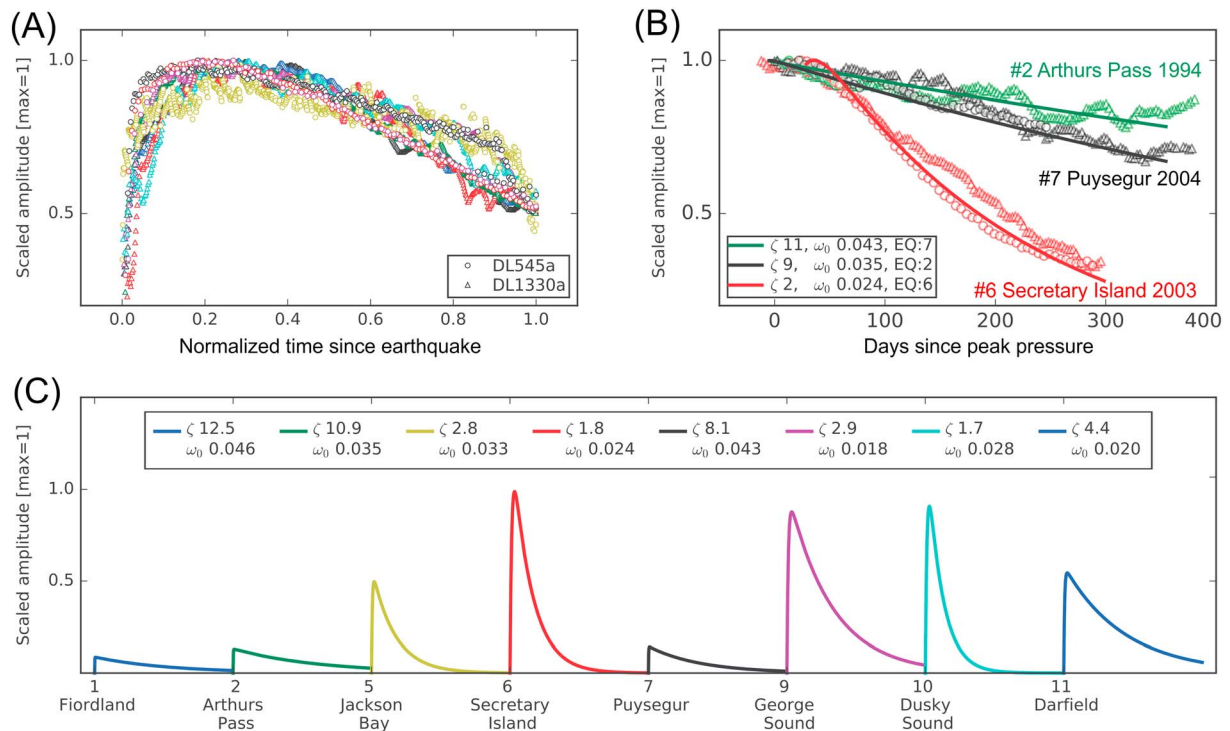
Figure 7. (a) Processed and absolute groundwater level changes extracted from wells DL545a (circles) and DL1330a (triangles) that have been scaled to maximum amplitude of 1 and normalized by the time to half recovery. Each color represents a different earthquake. (b) Damped harmonic oscillation models (equation (3)) showing differences in amplitude and recovery (time is normalized). For clarity, original 3 h daily data are plotted as selected weekly-monthly values. (c) Mean fit of the damped harmonic oscillator models derived at 22 piezometer sites for each earthquake.

The amplitudes of the hydrologic responses across all monitoring sites are also systematic (Figures 3 and 6). In nearly all cases, the maximum amplitude of groundwater level change at each site is that induced by the 2003 M_w7.0 Secretary Island earthquake; closely followed by the 2009 M_w7.8 Dusky Sound earthquake; then the 2007 M_w6.7 George Sound, 2010 M_w7.1 Darfield, M_w6.2 Jackson Bay, 2004 M_w7.1 Puysegur, 1994 M_w6.7 Arthurs Pass, and the 1993 M_w6.7 Fiordland earthquakes, respectively. By normalizing well-response amplitude to the maximum observed in response to an earthquake at any one site, or weir flow volume against the maximum weir change; then plotting against PGA we see, in general, only weak relationships between the relative amplitude of hydrological response and this measure for shaking intensity. A stronger but still diverse relationship is observed in weir data (Figures 6g–6i). Significant deviation from this trend relates to earthquakes with high PGA but shorter duration, narrower frequency bandwidth shaking, which induced relatively smaller responses. Time to peak pressure also appears to be related to PGA, but recovery time related more to the effect of earthquake shaking style.

The times to peak pressure and recovery of groundwater level changes also behave systematically (Figure 6). However, the recovery time follows a near-inverse pattern (Figure 6c) to that of amplitude: two of the three largest groundwater level change-inducing earthquakes (2003 M_w7.0 Secretary Island and 2009 M_w7.8 Dusky Sound earthquakes) exhibit relatively short recovery times, shorter than those to smaller responses (e.g., induced by the 1993 M_w6.7 Fiordland, 1994 M_w6.7 Arthurs Pass, and 2004 M_w7.1 Puysegur earthquakes). In contrast, responses to the 2001 M_w6.2 Jackson Bay, 2007 M_w6.7 George Sound, and 2010 M_w7.1 Darfield earthquakes had, with respect to their amplitude, relatively longer recovery periods.

The Spearman rank-order correlation matrices (Figures 6d–6f) reveal uniformly positive correlations, reflecting the extent to which the patterns in the amplitude of the earthquake-induced hydrological change throughout the gorge are systematic. Changes in weir flow rates and discharge volumes, although highly systematic, are more variable. This probably reflects the greater sensitivity of tunnel flow rate to rainfall "noise" than monitoring wells. The systematic patterns in earthquake-induced hydrologic responses suggest that the hydraulic behavior in Cromwell Gorge and the controls on it are congruent, and the ability of each hydrologic

system to resist and recover from change is affected by differences in the nature of earthquake-shaking within limits allowed by each local hydrologic system.

3.2. Hydrogeological Processes and the Effects of Geoengineering

Initial and long-term (ongoing) anthropogenic effects from the management of the landslide groundwater systems are apparent in the hydrological data. Three evolutionary trends in piezometer data from different sites can be recognized once the initial subsidence and recovery in response to gravity drainage, pumping, and the filling of the Lake Dunstan reservoir had ended. Water levels at each site are observed to have either maintained a consistent level, gradually risen, or gradually lowered. Tunnel weirs also exhibit one of the same three evolutionary trends in groundwater discharge, although some tunnels show greater sensitivity to rainfall and when this has been prolonged tend to mask any underlying long-term trend.

Four observations that provide insight into the effects of the geoengineering and hydrological processes occurring within the landslides are the following:

1. Long-term background trends do not appear to be altered by repeated earthquake stimulation (e.g., Figure 3b), suggesting that the volume of water available to move is limited by the storativity within each compartment and that different short- and long-term mechanisms are operating independently of each other.
2. The earthquake-induced groundwater level changes are temporary, and the polarities of these changes are not governed by whether the long-term landslide water levels are permanently in recovery or recession (Figure 3b), again reflecting separate, time-dependent mechanisms.
3. Earthquake-induced changes in tunnel discharge rates are always positive and occur on much shorter timescales than groundwater level changes (e.g., Figure 3c), indicating a disconnection between tunnels and monitored groundwater compartments and the effect of the "open" system generated by tunneling. The tunnels drain the downslope sections of the hydraulic gradients: thus, if permeability is enhanced, the tunnels would be expected to record an increase in discharge, even though much of this earthquake-released water is interpreted to come from the near-tunnel surface.
4. The landslide systems respond to earthquakes in a systematic manner (Figures 6d–6f), but responses to other external stimuli (e.g., storm events) and internal processes (e.g., those creating long-term changes) appear to be more random. External stimuli such as storms do not impart oscillatory ground motions in the same manner as an earthquake does and are not interpreted to have the ability to promote changes in hydraulic conductivity or permeability. However, rainfall-induced elevated piezometric levels have been observed to promote movement locally in some small parts of landslides [*Macfarlane*, 2009] by way of an increase in the hydraulic head of confined groundwater causing a decrease in local effective normal stress.

These four observations strongly suggest that the overall efficiency of the system and long-term processes that modulate it are not compromised by the temporary enhancement in fracture permeability induced by earthquakes. It appears likely that any temporary permeability enhancement occurring in fracture/shear zones is generated by a separate and independent mechanism to that causing the permanent slow increases and decreases in water levels and flow rates. Long-term alteration to groundwater flow (background trends) could, in Cromwell Gorge, be a result of geochemical processes such as precipitation and the growth of calcite cements and clays, as indicated by observations of calcite deposits on schist surfaces and tunnel walls, the periodic need for weirs to be cleaned of these and the lack of any significant structural deformation recorded in inclinometer and extensometer data.

3.3. Damped Harmonic Oscillation

Using a damped harmonic oscillator (DHO) model to quantify groundwater pressure evolution allows differences in the amplitude of changes induced at different sites, and corresponding variations in time to peak pressure and recovery, to be interpreted in terms of damping ratio and angular frequency, respectively. This approach scales the large variations observed in amplitudes and enables opposite polarities to be accommodated with a simple numerical model.

Results from the DHO modeling are illustrated in Figure 7. The upper left plot (Figure 7a) shows data from DL545a and DL1330a in the Nine Mile downstream slide area, which are examples of two end-member

responses. DL545a has meter-scale positive responses whereas DL1330a has centimeter-scale negative responses. The amplitudes are scaled to a maximum of 1, with negative responses from DL1330a converted to positive responses using absolute values, then aligned to a common start time and normalized by the time to half-recovery. Two subtly different groupings corresponding to larger and smaller groundwater level changes are evident, but given the scatter in these data, the responses are sufficiently similar that it is appropriate to model them in a common manner. The upper right plot (Figure 7b) shows the scaling distinguishes different earthquake responses regardless of site, despite major differences in sign and amplitude at DL545a and DL1330a, and the fitting of DHO models with different damping ratios and period. The optimal damping parameters and corresponding angular frequencies are determined for each earthquake-induced response at each site using a log-likelihood function, which returns the corresponding damping parameters and angular frequencies using a Gaussian distribution [O'Brien, 2014]. Mean values of ζ and ω_0 generated for each earthquake using all 22 piezometer sites with an observed response are illustrated in Figure 7c.

All modeled responses represent overdamped harmonic oscillation with estimated damping ratios consistently greater than 1 (Figures 7b and 7c). However, the amount of damping varies between earthquakes. The model parameters highlight differences in the recovery times of responses induced by earthquakes with comparable magnitudes throughout the monitoring wells. For example, the 2003 $M_w7.0$ Secretary Island, 2009 $M_w7.8$ Dusky Sound and 2007 $M_w6.7$ George Sound earthquakes consistently induce the three largest responses, but the 2003 $M_w7.0$ Secretary Island and 2009 $M_w7.8$ Dusky Sound earthquakes have smaller damping ratios (i.e., 1.8 and 1.7, respectively) reflecting quicker recovery than after the 2007 $M_w6.7$ George Sound earthquake (damping ratio of 2.9).

3.4. Seismological Characteristics of Earthquakes Triggering Hydrologic Responses

We have examined whether there was any systematic geometric relation between observed hydrological responses and earthquake focal mechanisms, directivity, and seismic wave arrival. The 11 earthquakes observed to have induced hydrological responses occurred at epicentral distances of 130–630 km (intermediate to far field), with shallow depths of 4–24 km and magnitudes of $M_w6.2$–7.8 (Figure 4 and summarized in Table 2). The earthquakes occurred at back-azimuths from Cromwell Gorge (i.e., gorge to earthquake) ranging from southwest to northeast, mostly in the locus of deformation along the active Pacific-Australian plate boundary zone. Little seismicity has occurred in the southeast quadrant with respect to the study area, which is furthest from the plate boundary and where deformation rates are lower. The P wave first motion focal mechanisms of the 11 earthquakes producing hydrologic responses are predominantly reverse with subsidiary strike-slip components (Figure 4). The raypaths corresponding to direct P waves propagating to the gorge generally, but not exclusively, plot in the compressional quadrant of the focal sphere or close to a nodal plane (Figure 4 inset stereonet). Conversely, the largest earthquake to have occurred during the analysis period which did not trigger a discernible hydrological response, the 2011 $M_w6.2$ Christchurch earthquake (Figure 4 earthquake 12), plots well within the dilatational quadrant of the focal sphere, within approximately 20° of the P axis. From this preliminary examination it seems plausible that P waves and directivity could potentially influence response triggering, but in this instance the distribution of earthquakes is not ideal so has not been further examined. Where earthquakes are more evenly distributed, this seems a worthy and fertile topic for investigation.

Measured and computed PGA and seismic energy density (e) values for earthquakes are listed in Table 2 and illustrated in Figure 8. For comparative purposes, all earthquakes recorded at EAZ seismometer (the nearest national broadband seismometer and strong motion site, installed in 2004) that did not induce hydrological responses within the Cromwell Gorge monitoring system are also shown, along with a compilation of world-wide examples of earthquake-induced water level changes in groundwater monitoring wells. Despite strong anthropogenic influence on absolute piezometric pressures, the stimulation of groundwater responses in the geoengineered landslides does not appear to be in any way abnormal (either sensitive or insensitive to earthquake energy).

Investigations into site-felt shaking intensity (Table 2) show that the monitored groundwater reservoirs experience/succumb to changes from quite low levels of shaking (measured PGA 0.1–1.45% g; equivalent to intensity less than Modified Mercalli Intensity MMIII) but are not particularly sensitive to faint earthquake shaking (e.g., PGA <0.1% g or teleseismic) compared with some world-wide examples (e.g., observation well
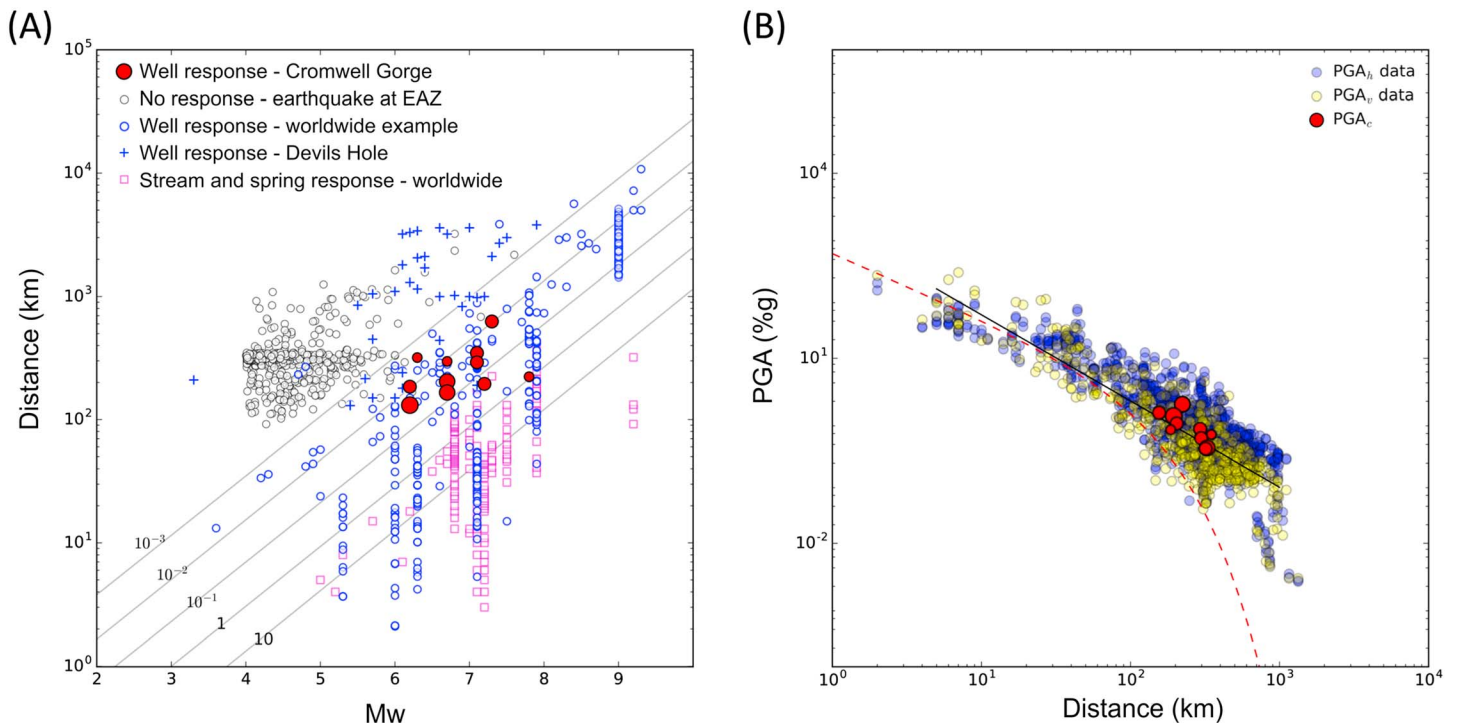
Figure 8. (a) Earthquake magnitude (M_w) plotted against epicentral distance showing the distribution of earthquake-induced hydrologic responses within Clyde Dam well and tunnel network in Cromwell Gorge (solid red circles scaled by approximate amplitude of the response), compared with black open circles depicting e values for all other New Zealand earthquakes recorded at EAZ seismometer since 2004 for which no discernable hydrological responses could be the Clyde Dam network. Comparable examples of wells (blue open circles) and stream responses (pink open squares) are also shown from worldwide compilations (data from *Wang and Manga* [2010], *Manga et al.* [2012], *Cox et al.* [2012, 2015], *Gulley et al.* [2013], *Shi et al.* [2013], *Shi and Wang* [2014], *Yan et al.* [2014], and *Zhang et al.* [2015]). Blue crosses distinguish the relatively anomalous sustained water level changes at Devils Hole [*Weingarten and Ge*, 2014]. Contours of constant seismic e in J m^{-3}, given by equation (2) are also shown to illustrate and compare cutoff values. (b) All recorded PGA vertical (yellow) and PGA horizontal (blue) at New Zealand strong motion sites (GeoNet) for the eight response-producing earthquakes since 2004. The calculated PGAc values (red) for shaking in Cromwell Gorge are shown along with equation (1) (black line) for a M_w 6.7, and the *Zhao et al.* [1997] model (red dash line).

27 F2 SOW 019, in Christiansburg, Virginia, and observations at Devils Hole; *Weingarten and Ge* [2014]). Measured PGA values suggest that a ground acceleration threshold in excess of 0.1% g is required to begin inducing some hydrological responses, with those observed associated with seismic energy density values larger than 0.13 J m^{-3}. However, based on eight earthquakes that produced a discernable response across all investigated monitoring wells and tunnel weirs, shaking intensity thresholds of at least 0.27% g PGA and an e value of at least 0.21 J m^{-3} are needed for widespread responses throughout Cromwell Gorge. This small variation in values reflects a combination of the degree of signal/noise in different landslide monitoring data as well as the variable response behavior of the landslides from one earthquake to the next.

The spectral characteristics of the 11 earthquakes that induced hydrological responses and a small number of those that did not have been categorized in terms of shaking duration, amplitude, and bandwidth in order to elucidate differences in earthquake-shaking style. Five categories of shaking can be identified, each of which contains two or more earthquakes: this suggests that the categories are robust and that different characters of earthquake shaking are repeated and potentially associated with different regions of the southern New Zealand plate boundary. The categories are defined in Table 3, and the earthquake spectra obtained via the continuous wavelet transform method are shown in Figure 9. The spectral categories correlate with the ability of each system to resist change, as modeled using the DHO (i.e., differences in the amplitude and duration of the response allowed by each system).

High-amplitude, long-duration (25–50 s or longer), and broad-bandwidth (1.5–2 orders of magnitude) shaking produced by the 2003 M_w7.0 Secretary Island and 2009 M_w7.8 Dusky Sound earthquakes (category 1) is associated with large responses that have relatively quick recovery (mean $\zeta < 1.8$ and $\omega_0 < 0.028$). In contrast, high-amplitude, short-duration (<25 s) narrow-bandwidth (<1 order of magnitude) shaking produced by the

Table 3. Spectral Categories Derived From the Continuous Wavelet Transform Plots in Figure 9

Category	Amplitude	Duration of High Amplitudes	Bandwidth (Orders of Magnitude)	Number of Earthquakes in Category
1	High	25–50+ s	1.5–2 orders	2
2	High	<25 s	Up to 1 order	2
3	Moderate	25–50 s	1.5–2 orders	3
4	Moderate	<25 s	Up to 1 order	2
5	Very low	<50 s	<2 orders	2

2001 M_w6.2 Jackson Bay and 2007 M_w6.7 George Sound earthquakes (category 2) is associated with large- or moderate-amplitude responses that recover more slowly (mean $\zeta < 2.9$ and $\omega_0 < 0.033$).

Moderate-amplitude, long-duration, broad-bandwidth shaking (1994 M_w6.7 Arthurs Pass, 2004 M_w7.1 Puysegur and 2010 M_w7.1 Darfield earthquakes; category 3) is associated with low-amplitude responses (mean $\zeta < 10.9$ and $\omega_0 < 0.043$) that recover quickly (although more slowly than for category 1 shaking). Moderate-amplitude, short-duration, narrow-bandwidth shaking (1993 M_w6.7 Fiordland and 2000 M_w6.2 Thompson Sound earthquakes; category 4) produced small hydrologic responses (mean $\zeta < 12.5$ and $\omega_0 < 0.046$) that recovered slowly. Finally, low-amplitude shaking, irrespective of duration and frequency-bandwidth, as generated by the 1995 M_w6.3 Cass and 2007 M_w7.3 Puysegur earthquakes (category 5), produces very small responses in small number of wells (i.e., not networkwide and therefore not included in the DHO modeling).

It is clear that in addition to the amplitude of shaking occurring at a site, the duration and bandwidth of shaking are key factors determining how groundwater will respond in the landslides.
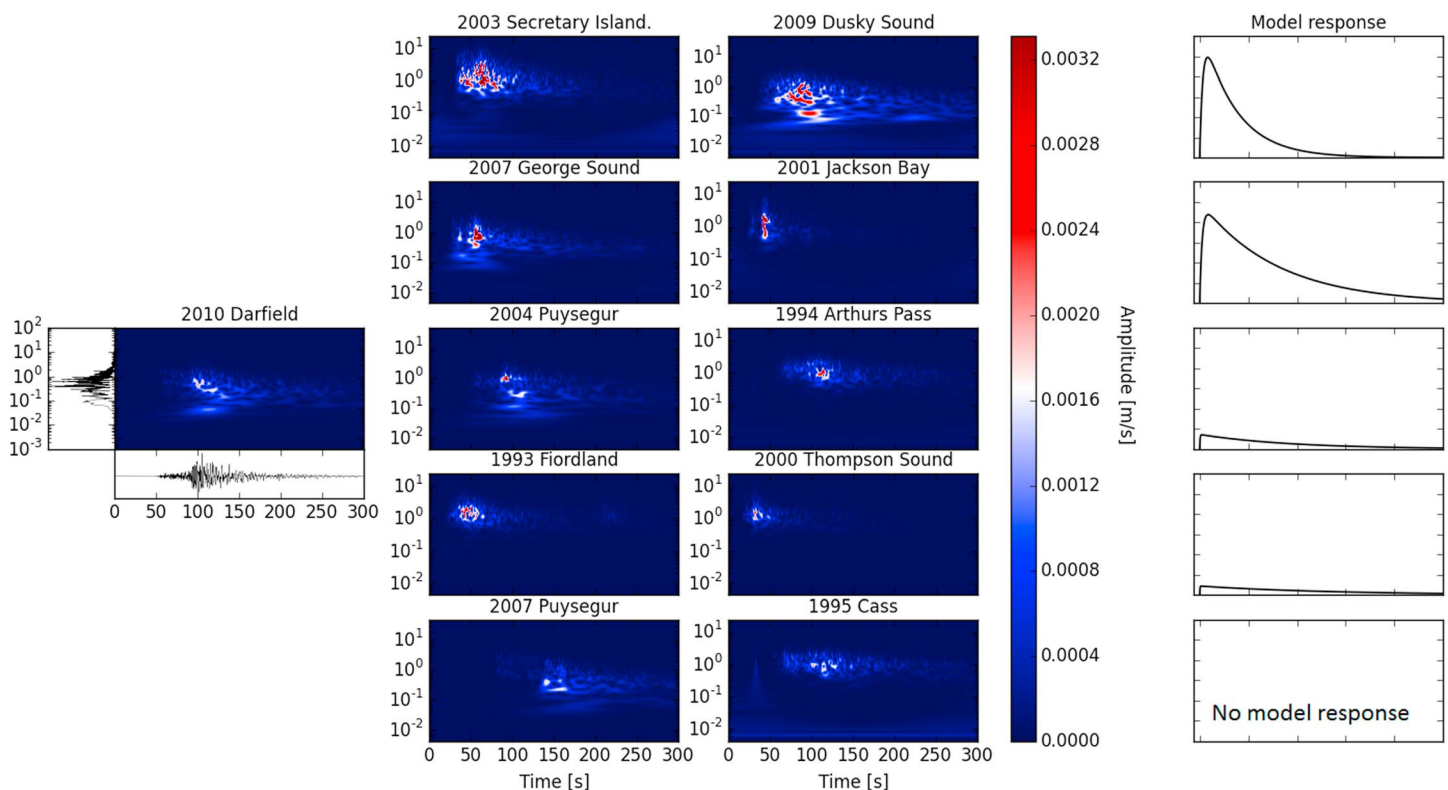

Figure 9. Continuous wavelet transforms plots, showing amplitude as a function of frequency (Hz; vertical axis) versus time (s), depicting differences in the earthquake energy at the closest seismometers to the study site. The plots are ordered into their respective spectral categories where the amplitudes are scaled to the total maximum, except for category 5, where 0.001 m/s has been added to enable visualization of the spectra. The model response plots on the far right depict the typical damped harmonic oscillator response modeled for each category, shown as scaled amplitude versus time.

4. Discussion

4.1. Landslide Hydrogeology and Mechanisms Invoking Change

Changes in groundwater level following earthquakes are relatively gradual and persistent in Cromwell Gorge and in many cases are of large amplitude compared with those reported in many other studies. Responses vary in polarity between different well locations and depths in the same landslide but are systematic from one earthquake to the next despite considerably different focal mechanisms. On this basis, some mechanisms commonly proposed to explain hydrological response to earthquakes can quickly be discounted in this case. For example, the local variations in polarity cannot be explained by volumetric strain associated with distal fault slip [e.g., *Ge and Stover*, 2000; *Jónsson et al.*, 2003; *Zhou and Burbey*, 2014]. With a lack of earthquake-related changes in extensometer and inclinometer data, or any detected motion requiring mitigation after intermediate and far-field earthquakes, the systematic hydrologic changes seem equally unlikely to be the result of volumetric strains associated with otherwise undetected movement of the now heavily engineered landslides. Instead, the local correlations between sites (e.g., Figure 2d) and delayed peak response and slow recovery within landslides, and the consistent release of water into tunnels, are consistent with some form of pressure equilibration between compartments in the fractured low-permeability landslide rock mass. The concept of earthquake-induced permeability enhancement [see *Manga et al.*, 2012], which is now widely proposed to explain hydrological responses to intermediate and far-field earthquakes [e.g., *Wang et al.*, 2004a, 2004b; *Shi and Wang*, 2014; *Weingarten and Ge*, 2014; *Shi et al.*, 2014, 2015a, 2015b; *Cox et al.*, 2015; *Wang and Manga*, 2015; *Zhang et al.*, 2015], seems directly applicable in Cromwell Gorge.

The degree of rock disturbance, groundwater pressure changes and groundwater flow are summarized in a general landslide model applicable in Cromwell Gorge (Figure 2). The groundwater regime within the landslides is complex and compartmentalized, involving limited transfer from higher-pressure and/or upslope compartments to lower pressure and/or downslope compartments, with flow concentrated through shear and crush zones, open faults, and areas of dilated, stress-relieved schist. We infer that distal earthquake shaking (dynamic stresses) above a $0.1\% g$ threshold enhances permeability and accentuates groundwater transfer and connectivity within fractures. Groundwater pressure may increase within confined reservoirs as oversteepened hydraulic gradients become more connected in upslope extensional landslide sections during flow pathway clearance yet remain less connected or confined in downslope compressional sections. Tunnels are located in the downslope, deeper sections of the landslides and in situ schist below basal shear zones and interact with the downslope extent of the hydraulic gradients. The rock mass that tunnels penetrate is saturated.

The earthquake-induced perturbations propagate rapidly (0–6 h.) within the open tunnel systems and are initiated effectively coseismically. In contrast the perturbations in the relatively closed parts of the landslide monitored by wells, also initiated coseismically, propagate more slowly (~700 h or 1 month). Earth tide responses occurring in both groundwater-level and tunnel flow data (e.g., Figures 3e and 3f where the S2, M2, K1, P1, and O1 phases have been picked in the frequency spectrum; for a full analysis see *O'Brien* [2014]) and hydraulic tests suggest the relatively slow response probably reflects the low hydraulic conductivities of the disturbed schist and groundwater compartmentalization. The more rapid response of flow into the tunnels is likely to reflect the modified stress regime surrounding the tunnels, where increases in near-tunnel surface storativity and hydraulic conductivity have been deliberately stimulated [*Beetham and Fergusson*, 1990].

Such changes in groundwater pressures and flow rates in response to earthquake perturbations can be conceptualized in two ways, using terminology from *McDonnell and Beven* [2014]: velocity-type responses, where amplitudes are controlled by the velocity of groundwater moving through subsurface flow paths, and celerity-type responses, defined by the speed at which a perturbation can propagate through the hydrogeologic system (resisted by inertia) such as a pressure wave from an increase in hydraulic head from rainfall. In this study we observe fundamental differences between hydrologic responses caused by rainfall events and those caused by earthquake perturbations. The speed at which earthquake-induced perturbations can propagate is envisaged to be controlled by the system's ability to resist hydraulic changes, but the extent to which earthquake-induced responses and equilibration might reflect altered celerity or velocity flow is difficult to fully quantify. Increases in groundwater flow velocity within fracture zones are apparent both within the tunnels, an open system where the distance from the tunnel wall to which the flow velocity increases is inferred to be more than tens of meters and between landslide reservoir compartments hundreds of meters apart that become connected as a result of earthquake stimulation (e.g., Figure 3d).

Differences in the perturbation time of the pressure wave in the tunnel weir data (from <6 h to ~1 month or approximately 1:200) and the well piezometer data (from 3 to 5 weeks to 0.7–1.2 years or approximately 1:12) are interpreted to reflect both the low hydraulic conductivities of the schist and local influence of the tunnel systems. The tunnel systems allow the rapid release of near tunnel-surface groundwater; quickly exhausting the immediate supply of water in large truncated fractures, but are replenished by groundwater flow through smaller fractures and from deeper within the rock mass. In contrast, major rainfall events recorded by tunnel weirs are seen to pass through the system much more slowly and are more subdued, involving ~2 months to peak flow rates followed by a 1 year recession, highlighting the effect of the dynamic stress imparted by the earthquakes.

Connectivity between and within groundwater compartments can be observed at some localities. For example, DL545a and DL692a (Nine Mile Downstream slide area) monitor subbasal groundwater and are 1052 m apart yet have nearly identical records: that is, the background hydrological signals (i.e., underlying trends), polarity, amplitude, and time-scales of groundwater level changes are highly similar, suggesting that the subbasal groundwater regimes these two monitoring wells sample are within the same compartment (or not compartmentalized). Another style of hydraulic relationship is demonstrated by monitoring wells (DL1204a and DL1206a), 95 m apart in the Clyde Slide, which have piezometers records that essentially mirror each other (Figure 3d). Here both wells monitor landslide-internal groundwater and record earthquake-induced changes in what we determine the characteristic manner for the gorge, with more pronounced changes induced by the Secretary Island M7.2 (earthquake 6) than the Puysegur M7.1 (earthquake 7). The total water level between the upslope (DL1206a) and downslope (DL1204a) compartments appears to be constant, perhaps indicating the earthquakes induce leakage of groundwater from DL1206a to DL1204a (perhaps in part emptying groundwater from upslope to downslope), or the earthquakes induce a change in the proportion of flow that causes different areas of the landslide to either preferentially recharge or discharge.

The observed consistency in the temporal nature of the closed systems˙ earthquake-induced responses is interpreted to reflect (1) congruent hydraulic properties (i.e., fracture-dominated permeability structure and hydraulic conductivity) of the landslide systems throughout the gorge, observed by the amplitude of the hydrograph (a velocity response) and (2) mechanical controls on the systems˙ abilities to resist and recover from change, seen in the time to and recovery from, peak-pressure change (a celerity response). Groundwater flow (i.e., velocity) and groundwater pressure transfer (i.e., celerity) are impeded within and across landslide hydrologic compartments by clayey gouges, calcite, and clay accumulations and coherent blocks of schist. Clayey gouge associated with crush and shear zones acts as an effective permeability barrier within these zones, restricting connectivity and increasing flow tortuosity. Gouge and calcite and clay accumulations are inferred to be relatively mobile and may be dislodged and translated during oscillatory shaking and subsequent increased flow velocities. Both precipitated and accumulated deposits of clay and calcite are found on tunnel walls and in weirs, but the extent to which they are physically accumulated or chemically precipitated is unclear.

Mechanical processes such as the opening and closing of fractures, flow path cleaning and physical transloca-tion of particulates, and potential creation of new fractures appear to be highly plausible processes in these landslides, occurring as a result of shaking and ground motion from distal earthquakes [e.g., *Manga et al.*, 2012]. Flow path cleaning by entrainment and translation of particulates, followed by particle settling out as flow becomes less turbulent, could happen rapidly within single fractures; but when scaled up to the extent the landslide systems, be prolonged. We cannot rule out the possibility that geochemical changes (dissolution and regrowth of calcite and clay cements) could play an important role in the enhancement and recovery of permeability [e.g., *Detwiler*, 2008; *Polak et al.*, 2003; *Yasuhara et al.*, 2006; *Bons et al.*, 2012; *Jones and Detwiler*, 2016], although we suspect this process occurs on a longer time-scale and is in part responsible for more gradual background trends (see below). The mixing of old and new groundwater has the potential to shift the chemical conditions forcing minerals in or out of solution but would require increased mixing and therefore, technically, be mechanically triggered.

4.2. Effects of Anthropogenic Geoengineering

Examples documented in this study reveal that the compartmentalized hydrological systems within the Cromwell Gorge landslides are remarkably dynamic on both long- and short-term timescales and encompass distinct, prolonged pressure changes that, when stimulated by seismic shaking, behave systematically and

consistently. Each landslide's hydrologic system has been, and continues to be, modulated by the geoengineering (e.g., gravity forced drainage, toe buttressing) to varying extents (i.e., different drainage capabilities). Notably, however, earthquake-induced changes in each landslide's hydrological state do not seem to correlate with the degree of anthropogenic modification of groundwater pressure, and although the peak ground accelerations that can stimulate change are relatively small, we have demonstrated that the associated seismic energies required to trigger a response are by no means abnormal or anomalous in an international context.

The groundwater levels (subbasal and internal) of all monitored sites were depressed by initial gravity drainage and pumping and are maintained below equilibrium levels due to the large-scale infrastructure. It is our expectation that the absolute amplitude of hydrological response to earthquakes, which are relatively large changes in comparison to those observed elsewhere, must therefore reflect the anthropogenic modification of the groundwater regime to some degree. However, once normalized, the proportional changes in groundwater level or weir flow rate increase show positive correlation with extrinsic parameters relating to the intensity and duration of shaking, so effects of anthropogenic modification appear to have been minimized or removed by this treatment of the data.

In contrast to the earthquake-induced responses, there is a much slower independent change (background trend) to the mass flux of water, which we interpret to be a consequence of geochemical processes slowly clogging the efficiency of the geoengineering and small volumetric stress changes associated with very slow landslide creep. Calcite and clays are found as young accumulations on tunnel walls and in weirs, and there is widespread evidence of surficial chemical weathering processes in Cromwell Gorge, including subsoil horizons comprised of leached calcite uncovered during engineering and the highly oxidized nature of near-surface schist [*Gillon and Hancox*, 1991]. It is possible that near-surface dissolution occurs and that dissolved minerals enter the landslides in more acidic infiltrating rainwater and then precipitate when mixed with older, more basic groundwater [cf., *Craw and Youngson*, 1993]. The slow volumetric stress changes associated with very slow landslide creep occur at a rate that remains partially detected by instrumentation and operational monitoring and appear totally independent of the dynamic effects of the distal earthquakes and their subsequent hydrological effects.

4.3. Overdamped Harmonic Oscillation

Viewing earthquake-induced hydrologic responses in relation to damped harmonic oscillation necessitates a change in how these phenomena are typically interpreted; the ability of the hydraulic system to resist change and then recover seems to be a dominant control of amplitude, polarity, and duration of hydrologic change. Differences in earthquake-shaking characteristics (i.e., intensity, duration, and frequency bandwidth) have a second-order effect, only altering the amplitude and duration of the response within the limits imposed by the groundwater regime and/or local hydrology. Crucially, once normalized, the earthquake-dependent second-order responses can reveal aspects regarding how the hydraulic properties (susceptible to change) of the rock mass become altered.

All modeled groundwater level changes within Cromwell Gorge represent overdamped harmonic oscillation, supporting the concept that the groundwater systems are able to resist some of the earthquake-induced changes over the time-scale of monitoring data. As yet there are no high-fidelity coseismic records available from Cromwell Gorge. Overdamped harmonic oscillation models the slow return of the system (recovering back to a prestimulated level) without oscillation or permanent alteration. The large delay in achieving peak pressure change, on the order of 1 month, also shows the degree of resistance, meaning that the corresponding changes are gradual. The observed delay to peak pressure is quite distinct from most observed intermediate to far-field responses and previously proposed modeling criteria [e.g., *Nespoli et al.*, 2016] for which groundwater responses are typically conceived as instantaneous peak-pore-pressure steps. The delay and amplitude must in part reflect the hydraulic conductivity of the systems and the scale of compartmentalization. This delay also implies a degree of disconnection between compartments (relatively closed systems) and tunnels (open systems), as tunnel interaction is seen to accelerate perturbations.

Large damping ratios (>4) reflect slow rates of groundwater level change (recovery), which we interpret as indicating a greater ability of the groundwater system to resist damage, and in contrast, small damping ratios (<4) reflect faster rates of change (recovery) and a lesser ability of the system(s) to resist damage. Differences in the groundwater level recovery time potentially provide insight into the relative degree of induced local

rock damage, that is, the dilation, unclogging, and/or generation of fracture(s). Shorter groundwater level recovery time signals faster transfer/dissipation of elevated pore pressures, and since the viscosity of the groundwater is not believed to decrease (rather increase during turbulent, particulate entraining fluid flow), is most likely a response to the degree of rock damage and/or flow pathway cleaning. The earthquake analysis shows that the groundwater level recovery times, and presumably processes causing them, are for the most part independent of PGA.

The underlying groundwater pressure appears to be an important factor in the ability of a hydrologic system to resist change but has no effect on the speed of change (i.e., celerity). Monitoring wells recording overpressured (i.e., above hydrostatic pressure) groundwater (common in confined reservoirs) observed the largest-amplitude groundwater level changes (e.g., nearly +7 m in DL545, Nine Mile Downstream slide area, where the piezometer level was decreased 130 m by drainage and after partial recovery now resides around 135 m below ground level; some 120 m above the sand filter and 80–100 m above the semipermeable basal shear zone), whereas wells monitoring unconfined (or perched) groundwater generally observed responses less than 1 m. Within the unconfined and/or perched reservoirs groundwater pressure does not immediately associate with the polarity of a response, which is determined by both the local hydraulic gradient and the effect of the drainage system(s). An increase in groundwater pressure may still result in a decrease in groundwater level if a low-pressure zone (created by forced drainage) in close proximity to a perched reservoir becomes connected.

4.4. Shaking Intensities and Spectral Characteristics

Robust relationships between earthquake shaking intensity measurements such as peak ground acceleration or derived peak ground velocity, Arias intensity, or seismic energy density with the amplitudes of hydrologic changes have been long sought-after. Compilations of international examples indicate that the intensity of earthquake shaking can be associated with the amplitude of hydrologic and/or hydraulic changes to a certain extent but is also influenced and complicated by local (intrinsic) geological and/or tectonic (extrinsic) factors [e.g., *Elkhoury et al.*, 2006; *Chia et al.*, 2008; *Manga et al.*, 2012; *Shi et al.*, 2015ab]. The combination of having multiple earthquakes with variable spectral characteristics and a dense array of response data in the relatively small area of Cromwell Gorge (approximately 70 km^2), normalized and modeled with a DHO in this study, enables us to reflect on the importance of earthquake spectra. Duration and frequency bandwidth seem to have a significant effect on the amplitudes and recovery times and are closely associated with ability of the groundwater regime in Cromwell Gorge landslides to resist and recover from change. Proportionally shorter recovery times of hydrologic responses in Cromwell Gorge are interpreted as proportionally greater increases in permeability, with flow and/or pressure wave transfer primarily through fracture networks in response to the increased unclogging/cleaning ability of analogies can be drawn between the cleaning effects of these oscillatory waves with those used in ultrasonic cleaning, where amplitude and frequency bandwidths are kept low and narrow to avoid cavitation damage [*Gale and Busnaina*, 1995] and in which the cleaning effect increases with the duration of excitation.

5. Conclusions

Comprehensive monitoring spanning a >20 year period at Cromwell Gorge, New Zealand, shows the partially drained and continually managed hill slopes and geoengineered landslides have hydrologic systems that are dynamic over both long- and short-term periods. We observe systematic (repeatable) large and small hydrologic responses occurring throughout various landslide groundwater systems (across ~18 km) to multiple intermediate to far-field earthquakes (>M_w 6.2). The originally slowly creeping schist landslides now have hydrologic systems altered by forced drainage and are continually modulated below equilibrium (potentiometric) levels but do not appear to be particularly sensitive to low-level seismic stimulation. In order to induce a widespread discernable response, threshold values of at least 0.27%g PGA and seismic energy density of 0.21 J m^{-3} need to be exceeded. Such thresholds are consistent with the majority of reported worldwide examples [e.g., *Manga et al.*, 2012], but many of the observed groundwater changes within the gorge are anomalously large (>1 m and as much as 6.9 m), and durations of both time to peak change and recovery (months to years) exceed those observed elsewhere, most likely reflecting the relatively low permeability (10^{-17} to 10^{-13} m^2) and internal structure of the landslides. Response amplitudes in part reflect the compartmentalization of hydraulic pressure and the surrounding hydraulic head that can become

connected during seismic shaking. Geoengineering likely influences the absolute scale of responses, although not their sensitivity to initiation.

Two distinct and characteristic earthquake-induced hydrologic responses were observed throughout the gorge, one associated with groundwater level changes observed in monitoring wells and the other with elevated groundwater discharge past underground V notch weirs. The changes are driven by dynamic stresses associated with the passage of seismic waves, and we envisage the mechanisms generating hydrologic change to involve fracture-scale permeability enhancement that is mostly mechanical. Using a damped harmonic oscillator to model the groundwater level changes enables conclusions to be drawn regarding the ability of the system to resist and recover from perturbations and highlights subtle differences in responses across different scales of amplitude (centimeter to meter scale) and polarity, which reveal similar patterns between earthquakes.

The fractured, compartmentalized (and in some cases overpressured) hydrologic systems exhibit resistance to change (i.e., damage) manifest as long delays in achieving peak pressure change and recovering. However, the hydrologic systems are notably more susceptible to change when stimulated with high-amplitude, long-duration, broad frequency bandwidth earthquake shaking, which corresponds to reduced damping ratios in an idealized damped harmonic oscillator model and indicate faster dissipation of elevated pore pressures via proportionally larger (although temporary) increases in fracture-dominated permeability. The close association of shaking duration and frequency bandwidth (that the landslides are subjected to) with the differences in amplitude and recovery time of the groundwater level changes (as allowed by the hydrologic system) emphasizes the effect that oscillatory waves can have on clogged hard-rock systems.

References

Abercrombie, R. E., T. H. Webb, R. Robinson, P. J. McGinty, J. J. Mori, and R. J. Beavan (2000), The enigma of the Arthur's Pass, New Zealand, earthquake: 1. Reconciling a variety of data for an unusual earthquake sequence, *J. Geophys. Res.*, 105, 16,119–16,137, doi:10.1029/2000JB900008.

Beetham, R., and D. Fergusson (1990), Clyde Power Station Reservoir, Nine Mile Slide (Downstream) engineering geological assessment. *Report EGI 89/041, Department of Scientific and Industrial Research*. Copy held in Contact Energy Library, Clyde Dam.

Beresnev, I. A., and P. A. Johnson (1994), Elastic-wave stimulation of oil production: A review of methods and results, *Soc. Explor. Geophys.*, 59, 1000–1017.

Blanchard, F. B., and P. Byerly (1935), A study of a well gauge as a seismograph, *Bull. Seismol. Soc. Am.*, 25, 313–321.

Bons, P. D., M. A. Elburg, and E. Gomez-Rivas (2012), A review of the formation of tectonic veins and their microstructures, *J. Struct. Geol.*, 43, 33–62, doi:10.1016/j.jsg.2012.07.005.

Brodsky, E. E., and L. J. Lajoie (2013), Anthropogenic seismicity rates and operational parameters at the Salton Sea geothermal field, *Science*, 341, 543–546.

Brodsky, E. E., E. Roeloffs, D. Woodcock, I. Gall, and M. Manga (2003), A mechanism for sustained groundwater pressure changes induced by distant earthquakes, *J. Geophys. Res.*, 108(B8), 2390, doi:10.1029/2002JB002321.

Burbey, T. J., D. Hisz, L. C. Murdoch, and M. Zhang (2012), Quantifying fractured crystalline-rock properties using well tests, earth tides and barometric effects, *J. Hydrol.*, 414–415, 317–328.

Candela, T., E. E. Brodsky, C. Marone, and D. Elsworth (2014), Laboratory evidence for particle mobilization as a mechanism for permeability enhancement via dynamic stressing, *Earth Planet. Sci. Lett.*, 392, 279–291.

Carrigan, C. R., G. C. P. King, G. E. Barr, and N. E. Bixler (1991), Potential for water table excursions induced by seismic events at Yucca Mountain, Nevada, *Geology*, 19, 1157–1160.

Chia, Y., J. J. Chiu, Y.-H. Chiang, T.-P. Lee, Y. M. Wu, and M.-J. Horng (2008), Implications of coseismic groundwater level changes onserved at multiple-well monitoring stations, *Geophys. J. Int.*, 172, 293–301.

Cox, S. C., H. K. Rutter, A. Sims, M. Manga, J. J. Weir, T. Ezzy, P. A. White, T. W. Horton, and D. Scott (2012), Hydrological effects of the M-W 7.1 Darfield (Canterbury) earthquake, 4 September 2010, New Zealand, *N. Z. J. Geol. Geophys.*, 55, 231–247.

Cox, S. C., C. D. Menzies, R. Sutherland, P. H. Denys, C. Chamberlain, and D. A. H. Teagle (2015), Changes in hot spring temperature and hydrogeology of the Alpine Fault hanging wall, New Zealand, induced by distal South Island earthquakes, *Geofluids*, 15, 216–239.

Craw, D., and J. H. Youngson (1993), Eluvial gold placer formation on actively rising mountain ranges, central Otago, New Zealand, *Sediment. Geol.*, 85, 623–635.

Daniel, W. W. (1990), Spearman rank correlation coefficient, in *Applied Nonparametric Statistics*, 2nd ed., pp. 358–365, PWS-Kent, Boston, Mass.

De Moortel, I., S. A. Munday, and A. W. Hood (2004), Wavelet analysis: The effect of varying basic wavelet parameters, *Sol. Phys.*, 222, 203–228.

Detwiler, R. L. (2008), Experimental observations of deformation caused by mineral dissolution in variable-aperture fractures, *J. Geophys. Res.*, 113, B08202, doi:10.1029/2008JB005697.

Elkhoury, J. E., E. E. Brodsky, and D. C. Agnew (2006), Seismic waves increase permeability, *Nature*, 441, 1135–1138.

Elkhoury, J. E., A. Niemeijer, E. E. Brodsky, and C. Marone (2011), Laboratory observations of permeability enhancement by fluid pressure oscillation of in situ fractured rock, *J. Geophys. Res.*, 116, B02311, doi:10.1029/2010JB007759.

Ellsworth, W. L. (2013), Injection-induced earthquakes, *Science*, 341(6142), doi:10.1126/science.1225942.

Faoro, I., D. Elsworth, and C. Marone (2012), Permeability evolution during dynamic stressing of dual permeability media, *J. Geophys. Res.*, 117, B01310, doi:10.1029/2011JB008635.

Fry, B., and M. C. Gerstenberger (2011), Large apparent stresses from the Canterbury earthquakes of 2010 and 2011, *Seismol. Res. Lett.*, 82, 833–838.

Fry, B., et al. (2010), The M_w7.6 dusky sound earthquake of 2009: Preliminary report, *Bull. N. Z. Soc. Earthquake Eng.*, *43*, 24–40.

Gale, G. W., and A. A. Busnaina (1995), Removal of particulate contaminants using ultrasonics and megasonics: A review, *Part. Sci. Technol.*, *13*, 197–211.

Ge, S., and S. C. Stover (2000), Hydrodynamic response to strike- and dip-slip faulting in a half space, *J. Geophys. Res.*, *105*(B11), 25,513–25,524, doi:10.1029/2000JB900233.

Gillon, M. D., and G. T. Hancox (1991), Cromwell Gorge landslides: A general overview, in *Landslides: Proceedings of the 6th International Symposium on Landslides*, vol. 2, edited by D. H. Bell, pp. 83–102, AA Balkema, Rotterdam, Netherlands.

Gillon, M. D., P. B. Riley, P. B. Lilley, and G. T. Hancox (1991), Movement history and infiltration, Cairnmuir Landslide, NZ, in *Landslides: Proceedings of the 6th International Symposium on Landslides*, vol. 2, edited by D. H. Bell, pp. 103–109, AA Balkema, Rotterdam, Netherlands.

Gledhill, K., R. Robinson, T. Webb, R. Abercrombie, J. Beavan, J. Cousins, and D. Eberhart-Phillips (2000), The M_w6.2 Cass, New Zealand, earthquake of 24 November 1995: Reverse faulting in a strike-slip region, *N. Z. J. Geol. Geophys.*, *42*, 255–269.

Gledhill, K., J. Ristau, M. Reyners, B. Fry, and C. Holden (2010), The Darfield (Canterbury, New Zealand) M_w 7.1 earthquake of September 2010: A preliminary seismological report, *Bull. N. Z. Soc. Earthquake Eng.*, *43*, 215–221.

Grocott, G. A., N. A. Crampton, R. J. De Luca, and P. J. Horrey (1992), Clyde Power Project Brewery Creek Slide Area: Geological and geotechnical assessment. Addendum A—Investigations and remedial works update Report EGI 89/016, Department of Scientific and Industrial Research. Copy held in Contact Energy Library, Clyde Dam.

Gulley, A. K., N. F. Dudley Ward, S. C. Cox, and J. P. Kaipio (2013), Groundwater responses to the recent Canterbury earthquakes: A comparison, *J. Hydrol.*, *504*, 171–181, doi:10.1016/j.jhydrol.2013.1009.1018.

Gurley, K., and A. Kareem (1999), Applications of wavelet transforms in earthquake, wind and ocean engineering, *Eng. Struct.*, *21*, 149–167.

Hill, D. P., et al. (1993), Seismicity remotely triggered by the magnitude 7.3 Landers, California, earthquake, *Science*, *260*, 1617–1623.

Jones, T. A., and R. L. Detwiler (2016), Fracture sealing by mineral precipitation: The role of small-scale mineral heterogeneity, *Geophys. Res. Lett.*, *43*, 7564–7571, doi:10.1002/2016GL069598.

Jónsson, S., P. Segall, R. Pedersen, and G. Björnsson (2003), Post-earthquake ground movements correlated to pore-pressure transients, *Nature*, *424*, 179–183.

Kaiser, A., et al. (2012), The M_w6.2 Christchurch earthquake of February 2011: Preliminary report, *N. Z. J. Geol. Geophys.*, *55*, 67–90.

Langridge, R. M., et al. (2016), The New Zealand active faults database, *N. Z. J. Geol. Geophys.*, *59*, 86–96.

Lay, T., and T. C. Wallace (1995), *Modern Global Seismology*, pp. 521, Academic Press, San Diego, Calif.

Liu, W., and M. Manga (2009), Changes in permeability caused by dynamic stresses in fractured sandstone, *Geophys. Res. Lett.*, *36*, L20307, doi:10.1029/2009GL039852.

Macfarlane, D. F. (2009), Observations and predictions of the behaviour of large, slow-moving landslides in schist, Clyde Dam reservoir, New Zealand, *J. Eng. Geol.*, *109*, 5–15.

Macfarlane, D. F., A. D. Pattle, and G. Salt (1991), Nature and identification of Cromwell Gorge landslide groundwater systems, in *Landslides: Proceedings of the 6th International Symposium on Landslides*, vol. 2, edited by D. H. Bell, pp. 509–517, AA Balkema, Rotterdam, Netherlands.

Manga, M., and J. C. Rowland (2009), Response of Alum Rock springs to the October 30, 2007 Alum Rock earthquake and implications for the origin of increased discharge after earthquakes, *Geofluids*, *9*, 237–250.

Manga, M., E. E. Brodsky, and M. Boone (2003), Response of streamflow to multiple earthquakes, *Geophys. Res. Lett.*, *30*, 1214, doi:10.1029/2002GL016618.

Manga, M., I. Beresnev, E. E. Brodsky, J. E. Elkhoury, D. Elsworth, S. E. Ingebritsen, D. C. Mays, and C.-Y. Wang (2012), Changes in permeability caused by transient stresses: Field observations, experiments, and mechanisms, *Rev. Geophys.*, *50*, RG2004, doi:10.1029/2011RG000382.

Matsumoto, N., G. Kitagawa, and E. A. Roeloffs (2003), Hydrological response to earthquakes in the Haibara well, central Japan—I. Groundwater level changes revealed using state space decomposition of atmospheric pressure, rainfall and tidal responses, *Geophys. J. Int.*, *155*, 885–898.

McDonnell, J. J., and K. Beven (2014), Debates—The future of hydrological sciences: A (common) path forward? A call to action aimed at understanding velocities, celerities and residence time distributions of the headwater hydrograph, *Water Resour. Res.*, *50*, 5342–5350, doi:10.1002/2013WR015141.

McGinty, P., R. Robinson, and T. Webb (2005), The 2001 ML 6.2 Jackson Bay earthquake sequence, South Island, New Zealand, *N. Z. J. Geol. Geophys.*, *48*, 315–324.

Nespoli, M., M. Todesco, E. Serpelloni, M. E. Belardinelli, M. Bonafede, A. Marcaccio, A. P. Rinaldi, L. Anderlini, and A. Gualandi (2016), Modelling earthquake effects on groundwater levels: Evidences from the 2012 Emilia earthquake (Italy), *Geofluids*, *16*, 452–463, doi:10.1111/gfl.12165.

O'Brien, G. (2014), Earthquake-induced hydrologic changes in the geoengineered schist landslides of Cromwell Gorge, central Otago. Unpublished MSc thesis, pp. 150, Victoria Univ. of Wellington, New Zealand.

Okada, Y. (1992), Internal deformation due to shear and tensile faults in a half-space, *Bull. Seismol. Soc. Am.*, *82*, 1018–1040.

Parvin, M., N. Tadakuma, H. Asaue, and K. Koike (2014), Delineation and interpretation of spatial coseismic response of groundwater levels in shallow and deep parts of an alluvial plain to different earthquakes: A case study of the Kumamoto City area, southwest Japan, *J. Asian Sci.*, *83*, 35–47.

Petersen, T., et al. (2009), The M_w 6.7 George Sound earthquake of October 15, 2007: Response and preliminary results, *Bull. N. Z. Soc. Earthquake Eng.*, *42*, 129–141.

Polak, A., D. Elsworth, H. Yasuhara, A. S. Grader, and P. M. Halleck (2003), Permeability reduction of a natural fracture under net dissolution by hydrothermal fluids, *Geophys. Res. Lett.*, *30*(20), 2020, doi:10.1029/2003GL017575.

Polak, A., D. Elsworth, J. Liu, and A. Grader (2004), Spontaneous switching of permeability changes in a limestone fracture under net dissolution, *Water Resour. Res.*, *40*, W03502, doi:10.1029/2003WR002717.

Reyners, M. (2011), Lessons from the destructive M_w 6.3 Christchurch, New Zealand, earthquake, *Seismol. Res. Lett.*, *82*, 371–372.

Reyners, M., et al. (2003), The M_w 7.2 Fiordland Earthquake of August 21, 2003: Background and Preliminary Results, *Bull. N. Z. Soc. Earthquake Eng.*, *36*, 233–248.

Robinson, R., T. Webb, P. McGinty, J. Cousins, and D. Eberhart-Phillips (2003), The 2000 Thompson Sound earthquake, New Zealand, *N. Z. J. Geol. Geophys.*, *46*, 331–341.

Roeloffs, E. (1998), Persistent water level changes in a well near Parkfield, California, due to local and distant earthquakes, *J. Geophys. Res.*, *103*, 869–889, doi:10.1029/97JB02335.

Rojstaczer, S., S. Wolf, and R. Michel (1995), Permeability enhancement in the shallow crust as a cause of earthquake-induced hydrological changes, *Nature*, *373*, 237–239.

Shi, Z., and G. Wang (2014), Hydrological response to multiple large distant earthquakes in the Mile well, China, *J. Geophys. Res. Earth Surf.*, *119*, 2448–2459, doi:10.1002/2014JF003184.

Shi, Z., G. Wang, C. Liu, J. Mei, J. Wang, and H. Fang (2013), Coseismic response of groundwater level in the Three Gorges well network and its relationship to aquifer parameters, *Chin. Sci. Bull.*, *58*, 3080–3087.

Shi, Z., G. Wang, C.-Y. Wang, M. Manga, and C. Liu (2014), Comparison of hydrological responses to the Wenchuan and Lushan earthquakes, *Earth Planet. Sci. Lett.*, *391*, 193–200.

Shi, Z., G. Wang, M. Manga, and C.-Y. Wang (2015a), Mechanism of co-seismic water level change following four great earthquakes—Insights from co-seismic responses throughout the Chinese mainland, *Earth Planet. Sci. Lett.*, *430*, 66–74.

Shi, Z., G. Wang, M. Manga, and C.-Y. Wang (2015b), Continental-scale water-level response to a large earthquake, *Geofluids*, *15*, 310–320.

Sibson, R. H. (2001), Seismogenic framework for hydrothermal transport and ore deposition, *Soc. Econ. Geol. Rev.*, *14*, 25–50.

Taira, T., P. G. Silver, F. Niu, and R. M. Nadeau (2009), Remote triggering of fault-strength changes on the San Andreas fault at Parkfield, *Nature*, *461*, 636–640.

Tamura, Y., and D. Agnew (2008), Revised Baytap08 user manual. *Scripps Institution of Oceanography Technical Report*.

Tamura, Y., T. Sato, M. Ooe, and M. Ishiguro (1991), A procedure for tidal analysis with a Bayesian information criterion, *Geophys. J. Int.*, *104*, 507–616.

Thomson, R. (1993), Clyde Dam engineering geological completion report. *Unpublished Contract Report C-1992/18 Clyde Power Project*. *Held in GNS Science library*. [Available at www.gns.cri.nz.]

Turnbull, I. M. (1987), Sheet 133 Cromwell: Geological map of New Zealand. 1:63,360 Sheet S133. *Department of Scientific and Industrial Research*, *Wellington*, *New Zealand*.

Turnbull, I. M., N. Mortimer, and D. Craw (2001), Textural zones in the Haast Schist—A reappraisal, *N. Z. J. Geol. Geophys.*, *44*, 171–183.

van Dissen, R., J. Cousins, R. Robinson, and M. Reyners (1994), The Fiordland earthquake of 10 August, 1993: A reconnaissance report covering tectonic setting, peak ground acceleration, and landslide damage, *Bull. N. Z. Soc. Earthquake Eng.*, *27*, 147–154.

Wang, C.-Y. (2007), Liquefaction beyond the near field, *Seismol. Res. Lett.*, *78*, 512–517.

Wang, C.-Y., and M. Manga (2010), Hydrologic responses to earthquakes and a general metric, *Geofluids*, *10*, 206–216.

Wang, C.-Y., and M. Manga (2015), New streams and springs after the 2014 M_w6.0 South Napa earthquake, *Nat. Commun.*, *6*, 7597, doi:10.1038/ncomms8597.

Wang, C.-Y., M. Manga, D. Dreger, and A. Wong (2004a), Streamflow increase due to rupturing of hydrothermal reservoirs: Evidence from the 2003 San Simeon, California, Earthquake, *Geophys. Res. Lett.*, *31*, L10502, doi:10.1029/2004GL020124.

Wang, C.-Y., C.-H. Wang, and M. Manga (2004b), Coseismic release of water from mountains—Evidence from the 1999 ($M_w = 7.5$) Chi-Chi, Taiwan, earthquake, *Geology*, *32*, 769–772.

Weingarten, M., and S. Ge (2014), Insights into water level response to seismic waves: A 24-year high-fidelity record of global seismicity at Devils Hole, *Geophys. Res. Lett.*, *41*, 74–80, doi:10.1002/2013GL058418.

Wilson, S., and X. Lu (2011), *Rainfall Recharge Assessment for Otago Groundwater Basins*, Otago Regional Council, Dunedin, ISBN:978-970-478-37621-37620.

Wylie, C. R., and L. C. Barrett (1995), *Advanced Engineering Mathematics*, 6th ed., McGraw-Hill Publishing Company, New York.

Yan, R., H. Woith, and R. Wang (2014), Groundwater level changes induced by the 2011 Tohoku earthquake in China mainland, *Geophys. J. Int.*, *199*, 533–548.

Yasuhara, H., A. Polak, Y. Mitani, A. Grader, P. Halleck, and D. Elsworth (2006), Evolution of fracture permeability through fluid-rock reaction under hydrothermal conditions, *Earth Planet. Sci. Lett.*, *244*, 186–200, doi:10.1016/j.epsl.2006.01.046.

Zhang, Y., L.-Y. Fu, F. Huang, and X. Chen (2015), Coseismic water-level changes in a well induced by teleseismic waves from three large earthquakes, *Tectonophysics*, *651-652*, 232–241.

Zhao, J. X., D. J. Dowrick, and G. H. McVerry (1997), Attenuation of peak ground accelerations in New Zealand earthquakes, *Bull. N. Z. Soc. Earthquake Eng.*, *30*, 133–158.

Zhou, X., and T. J. Burbey (2014), Pore-pressure response to sudden fault slip for three typical faulting regimes, *Bull. Seismol. Soc. Am.*, *104*, 793–808.